Development of a DNA-based Aptasensor for Rapid Detection of Tuberculosis

By

Reem Ahmed Karaballi

A Thesis Submitted to
Saint Mary's University, Halifax, Nova Scotia
In Partial Fulfillment of the Requirements for the Degree of
Bachelor of Science with Honours in Chemistry

April 2013, Halifax Nova Scotia

Approved: Dr. Christa L. Brosseau
Supervisor

Approved: Prof. Mary Sheppard
Examiner

Approved: Dr. Jason D. Masuda
Examiner

Date: April 25, 2013

Certification

Development of a DNA-based Aptasensor for

Rapid Detection of Tuberculosis

I hereby certify that this thesis was completed by Reem Ahmed Karaballi in partial fulfillment for the requirements of the Degree of Bachelor of Science with Honours in Chemistry at Saint Mary's University and I certify that this is truly the original work carried out by Reem Ahmed Karaballi.

Thesis Supervisor

   Dr. Christa L. Brosseau

Chairperson of the Chemistry Department

   Dr. Kathy L. Singfield

Dean of Science

   Dr. Steven M. Smith

ABSTRACT

Development of a DNA-based Aptasensor for Rapid Detection of Tuberculosis

By Reem Karaballi

This project focuses on the development of a portable DNA-aptamer based biosensor, which is referred to as an aptasensor, that would aid in the diagnosis of the highly contagious disease tuberculosis. An important aspect of this project is to obtain a signal for DNA using electrochemical surface-enhanced Raman spectroscopy (E-SERS), with an aptamer used to bind specific biomarkers for detection. This method was used to detect the signal of DNA bases, nucleotides, and an oligonucleotide. Screen printed electrodes modified with silver colloidal nanoparticles were immersed in the DNA base and nucleotide solutions. A voltage was applied varying from 0.0 to -1.0V. These experiments showed that DNA components can be detected using E-SERS. Several molecules were tested as possible choices for backfilling, in order to prevent surface denaturation of the DNA and to reduce non-specific binding. Signal was detected for the aptamer (referred to as probe 1), and hybridization studies between probe 1 and its complimentary sequence, target 1, were successful using 12-mercaptododecanoic acid as the backfilling spacer. The limit of detection for the target on the SERS substrate used was found to be approximately 0.4 mM. The ds-DNA TB oligo was weakly detected after the modification of the AgNP electrode using 0.5 M KCl. These results indicate that a SERS-based aptasensor has great potential in the field of rapid diagnostics.

April 25, 2013.

Dedication

I would like to dedicate this thesis to my family and friends who stood by my side

through the good and bad.

Acknowledgments

I would like to thank my supervisor Dr. Christa L. Brosseau for allowing me to work in her research lab, and for accepting me as an honours student. She has been very helpful with guiding me through this project, so that I have both achieved my goals and learnt a lot along the way. I would like to thank my group members: Osai Clarke, Ashley Robinson, Scott Harroun, Soraya Merchant. I would like to thank my other friends in the Department of Chemistry, for their support and encouragement. Also, I would like to extend great thanks to my family and friends for supporting throughout this journey.

Finally I would also like to thank Andrew Nel, of the Dr. Jonathan Blackburn group at the University of Cape Town for working on the DNA aptamers and the TB oligo and providing helpful information. Additionally, I would also like to thank all of the Department of Chemistry Faculty and Staff. Without having received such a sound education in the field of chemistry, I could never have dreamed of undertaking a work such as this presented herein.

Lastly, I would like to thank my family and friends have been very supportive of my educational goals, and their support has been much appreciated.

Table of Contents   **page**

Table of Contents Continued **page**

Table of Contents Continued **page**

List of Figures   Page

List of Figures continued

List of Tables   page

List of Abbreviations

POC   point-of-care

AgNP   silver nanoparticles

TB   tuberculosis

M.Tb.   *Mycobacterium tuberculosis*

MTBC   M.Tb. complex

DNA   deoxyribonucleic acid

ss-DNA   single-stranded deoxyribonucleic acid

ss-RNA   single-stranded ribonucleic acid

anti VEGF   antivascular endothelial growth factor

SELEX   systematic evolution of ligands by exponential enrichment

PCR   polymerase chain reaction

pLDH   *Plasmodium* lactate dehydrogenase

PvLDH   *Plasmodium vivax* LDH

PfLDH   *Plasmodium falciparum* LDH

EIS   electrochemical impedance spectroscopy

tr-DNA   trans-renal DNA

MGEs   mobile genetic elements

IS   insertion sequence

DR   direct repeats

RFLP   restriction fragment length polymorphism

RE   reference electrode

CE   counter electrode

WE   working electrode

CV   cyclic voltammetry

IR   Infrared spectroscopy

List of Abbreviations continued

SERS   surface-enhanced Raman spectroscopy

LSPR   localized surface plasmon resonance

E-SERS   electrochemical surface-enhanced Raman spectroscopy

SSR   surface selection rule

TMR   tetramethylrhodamine

3-MPA   3-mercaptopropionic acid

OCP   open circuit potential

dAMP   2'-deoxyadenosine 5'-monophosphate

dCMP   2'-deoxycytidine 5'-monophosphate

dTMP   thymidine 5'-monophosphate

dGMP   2'-deoxyguanosine 5'-monophosphate

SAM   self-assembled monolayer

12-MDA   12-mercaptododecanoic acid

ds-DNA   double-stranded DNA

TB Oligo.   tuberculosis oligonucleotides

Fwhm   full width at half maximum

SPE   screen printed electrode

Chapter 1: Introduction

1.1 Introduction

Many areas in research today are focused on finding ways of pre-determining diseases that have a negative impact on human health. Currently it is possible to diagnose specific diseases using devices that detect a biomarker pertaining to the disease in bodily fluids. Some examples include diabetes and prostate cancer.[1,2] In developing nations, thousands of largely preventable deaths occur every year due to diseases that are unable to be diagnosed or treated in a timely manner. Three diseases for which rapid diagnosis is not currently available in resource-limited settings are tuberculosis, malaria, and HIV; these diseases predominantly occur in Sub-Saharan Africa. In order to rapidly detect these diseases, a point-of-care (POC) diagnostic platform is needed. This POC device will help to rapidly diagnose a disease or host of diseases wherever the patient is being treated. Some desirable characteristics that such a device should possess include a fast response time, an easily interpreted signal, portability, ruggedness and the ability to detect an analyte present at low concentration, use of disposable chips or strips, and finally the device should be cost-effective.[3] In addition, there are many challenges one faces when developing such a device for use in developing nation settings, such as conditions of high temperature and humidity, limited access to clean water, operator illiteracy, and an unstable or non-existent source of electricity.

This research focuses on developing a novel POC device to detect specific biomarkers that are indicative of tuberculosis (TB). Until now, there is no accurate or reliable method to provide a fast positive response for tuberculosis patients. Once

developed, this device will be referred to as an aptasensor, since specifically designed nucleic acids, called DNA aptamers, will be used as the receptors on the surface of the device specifically to bind tuberculosis biomarkers. The DNA aptamers will be present on the surface of an electrode containing colloidal silver nanoparticles. Surface-enhanced Raman spectroscopy coupled with electrochemistry (E-SERS) will be used to detect the signal of the aptamer and bound biomarker.

The overall goal of this research project is to develop an E-SERS based sensor that uses DNA aptamers for selective detection of disease biomarkers at the POC. The first step was to characterize the signal for DNA bases and DNA nucleotides, which will help to identify and distinguish the vibrational features of each base and nucleotide from one another. Next, single-stranded DNA aptamers were investigated on both modified and an unmodified silver nanoparticle (AgNP) electrode surface. Finally, the conclusion of this project sought to model the selective binding of DNA fragments from *Mycobacterium tuberculosis* (*M.tb.*) to the DNA-aptamers functionalized onto the electrode surface as proof of concept for rapid TB detection.

1.2 Literature Review:

1.2.1 Tuberculosis

Tuberculosis (TB) is a common, and often lethal, highly infectious disease caused by the bacterium *Mycobacterium tuberculosis* (*M.tb.*).[4] *M.tb.* was discovered in 1882 by Robert Koch, and was described as a long, slender, rod-shaped bacterium, with a slow growth rate.[5] *M.tb.* belongs to a group known as *M.tb. complex (MTBC)*, which contains six other organisms that are closely related: *M. bovis, M. africanum, M. pinnipedii, M.*

caprae, M. microti, and M. canetti.[6] *M.tb.* can affect any part of the human body, such as the brain, kidney, spine, and especially the lungs because it requires oxygen for its growth.[7] Even though this bacterium is the cause of TB disease, it can still be present in a host body without the host becoming symptomatic. However, if an active TB infection is present, it can be easily spread among people by coughing, sneezing, or even by talking, which is why TB is considered to be an airborne disease.[8] While TB can affect anyone, active TB cases are most common for people in close contact with TB patients, such as those that work in care facilities, people infected with HIV, the young and elderly, and those living in poorer regions. In South Africa, 21% of all deaths are due to TB, and 70% of TB patients are also HIV positive.[9] Some of the symptoms that active TB patients experience include fever, night sweats, weight loss, chest pains, and coughing up blood or sputum.[4,8] Currently one third of the world's population is infected by latent TB, and according to the World Health Organization, active TB results in two million deaths annually.[10,11]

In developed countries, TB is commonly diagnosed using chest X-rays, blood samples, and also through skin tests. The skin test that is commonly used is referred to as the Mantoux skin test, which consists of injecting a small amount of purified protein derivative tuberculin into the skin of the forearm. The results are then determined based on the skin reaction that occurs within 48-72 hours.[11] Any redness or swelling of the skin indicates a positive test for TB; however, these results do not determine if it is an active or latent TB infection. Also, this test can lead to false-positives or false-negatives, which would need further tests.[11] This test is not used in third world countries due to their

limited availability of resources. The main methods that are currently used to detect TB in South Africa are smear microscopy and culture studies.[12] Smear microscopy is used to identify the bacteria that are present in body fluid samples, such as sputum, by staining the *M.tb* using an acid-fast stain. This test is done on *M.tb* because the bacterium contains a waxy layer around the cell due to the presence of mycolic acid on the cell walls.[5] The sputum sample suspected of containing the *M.tb* is smeared on a slide, and then stained first by carbolfuchsin, a red dye. The slide is heated to make sure the dye penetrates the *M.tb*, and then it is usually rinsed with acid-alcohol after the slide is cooled. The sample is then stained with methylene blue as a counterstain. Cells that contain the waxy layer will appear red and are considered acid-fast, and cells that absorb the counterstain will be considered not acid-fast.[5] In South Africa, these studies usually take between 4-16 weeks to provide results to the patient, which is problematic since ~40% of patients never return to the clinic for their diagnosis or treatment.[9] All of these statistics suggests that a rapid-sensing device should be developed to detect tuberculosis biomarkers at or near the point-of-care as a way to improve global healthcare.

1.2.2 DNA

Deoxyribonucleic acid (DNA) exists in a double helix structure and carries the genetic information found in living organisms. The structure basically consists of four different nucleotide bases which are adenine (A), guanine (G), cytosine (C), and thymine (T). These heterocyclic nitrogenous bases are usually linked to a five-carbon sugar through a glycosidic bond which forms compounds called nucleosides. The sugar present in the nucleosides is a 2'deoxyribose, which has one –OH group that is available for the

esterification of the phosphoric acid to the sugar. This esterification causes the addition of a phosphate group on the 5' or 3' position of a sugar that already contains one of the four bases, which can result in the formation of nucleotides.[13] The nucleotides of a single-stranded DNA are linked together in a polynucleotide chain through 3', 5'-phosphodiester bridges. A polynucleotide strand is found to bind specifically only to its complementary strand through interchain hydrogen bonds between the pyrimidine and purines. In 1953, Watson and Crick studied the structure of the DNA helix using X-ray diffraction which led to the "Watson-Crick" model of base pairing where A binds to T, and G binds to C as shown in Figure 1 below.[13]
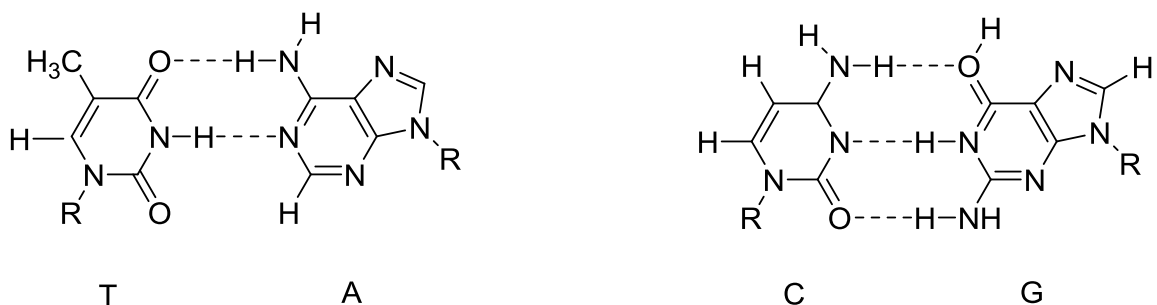
Figure 1: Base-pairing between the four DNA bases: T and A, C and G.

The hybridization of one DNA strand with its complementary strand is very important in the development of DNA-based sensors. There have been some techniques used for detecting DNA sequences using radioactive labels which are now being replaced by non-radio isotopic labels, such as fluorescent dyes, chemiluminescent agents, digoxigenin, and avidin/biotin.[14] These techniques might have many interesting applications; however, the disadvantage in using them is that they involve labeling and tagging the DNA. These methods decrease the performance of DNA probes, have low

sensitivity, require a lot of work and training, and the instruments are relatively expensive.[15] Scientists have increasingly been more interested in label-free DNA detection methods using electrochemical methods such as voltammetry, impedance spectroscopy, amperometry, and even well-known vibrational spectroscopic methods like Raman spectroscopy.[16]

1.2.3 DNA Aptamers

Over twenty years ago, aptamers were independently described by three groups as nucleic acid macromolecules of artificial single-stranded DNA or RNA sequences (ss-DNA, ss-RNA).[17-19] These nucleic acid aptamers are capable of adopting stable secondary and tertiary structures, which enables specific interactions with other molecules.[20,21] Aptamers are specially engineered to bind specifically to a target molecule, such as a protein, glycolipid, small molecule, or another DNA fragment.[22,23] In addition, aptamers have high binding affinities in the nanomolar to picomolar range for large molecules, and in the micromolar range for small molecules.[21,24,25]

DNA aptamers have recently been used in numerous analytical and biological applications for diagnostic purposes such as target capture, cell imaging, drug delivery, molecular sensing, and selective chromatography.[21] In the literature, aptamers are widely used as a targeting modality to bind to therapeutic targets such as IgE, alpha-thrombin, IFN-g, and PTPase, cancer cells, and influenza virus H1N1.[25-27] The most common aptamer-based application that is currently being used in clinics is in the treatment of age-related macular degeneration, which uses an antivascular endothelial growth factor (anti-VEGF) aptamer. VEGF 165 promotes the growth of abnormal new

6

blood vessels in the eyes, which leads to blood leakage and eventual vision loss. This aptamer is injected into the patient's vitreous cavity to bind to the target, which will inhibit the binding between the target and its receptor. More than 80% of patients noticed improvements in their vision within months of being treated, and now the aptamer has been fully approved by the US Food and Drug Administration and is commercially referred to as Pegaptanib® or Macugen®.[25, 28,29]

In order for aptamers to achieve high sensitivity and selectivity, they should be processed very carefully. In 1990, Gold[17] and Szostak[18] independently discovered a method for preparing nucleic acid aptamers by an *in vitro* selection process called systematic evolution of ligands by exponential enrichment (SELEX).[23,28] The idea of the SELEX method was developed using the concept of natural evolution, which results in three steps that include diversification, selection and replication.[28] This technique starts by building a random library containing 10^{13}-10^{15} ss-DNA sequences.[21,23] Each DNA sequence usually varies in the number of nucleotides present. According to the literature; however, an ideal sequence usually contains between 20-90 nucleotides.[20,28] These DNA sequences usually contain two regions, a middle region containing a random sequence, and fixed regions on the 3' and 5' ends. The fixed regions are usually flanked by a known primer sequence that often contains between 15-30 nucleotides to enable polymerase chain reaction (PCR) amplification.[28,30] The initiation step to start the cycle of selection is to incubate the library of the ss-DNA in the target of interest (Figure 2). [21] This would cause some of the ss-DNA aptamers to bind to the target, while others remain unbound or weakly-bound.[20] There are some methods that have been used for separating

the bound aptamers from the unbound, while at the same time ensuring purity and selectivity. For example, affinity chromatography, flow cytometry, capillary electrophoresis, plasmon resonance, and filtration through nitrocellulose have all been explored for separation.[21] The second step is to elute these bound aptamers by using high salt, temperature, chaotropic agents, or any other factor that would be able to disrupt the molecular interactions between the target and the aptamer.[20] These eluted aptamers will then be amplified by PCR using primers complementary to the flanking sequence in the ss-DNA.[20] This cycle then repeats between eight and 15 times for affinity selection and amplification of the aptamer that binds best to the target, and to eliminate any non-specific binding.[23,30] The aptamers are then cloned to identify their sequence and the binding species.[20,23] These aptamers are then used to selectively detect the target molecule.
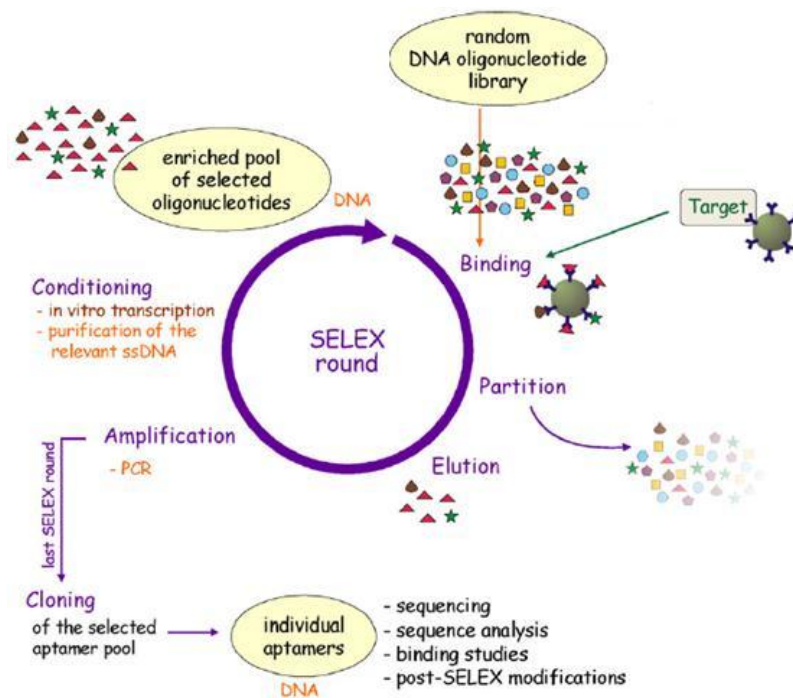
Figure 2: Representation of the SELEX process for the selection of DNA aptamers. Reproduced with permission.[31]

Although this powerful technique was the first method used for selection of aptamers and it remains in use today, a major limitation was that it required six-eight weeks to complete the process. As a result, the SELEX process had to undergo modification and refinement to increase the speed and simplicity of production. SELEX can be coupled with other techniques such as photo-SELEX, capillary electrophoresis-SELEX, and microfluidic-SELEX.[20,21,23] There are also non-SELEX techniques for aptamer selection such as capillary electrophoresis and non-equilibrium capillary electrophoresis of an equilibrium mixture.[20,21]

1.2.4 Aptasensor

There has been huge growth in the development of sensors over the last several decades. Some examples include potentiometric sensors, voltammetric sensors, conductometric sensors, amperometric sensors, mass sensors, immunosensors and biosensors.[32,33] A biosensor is a device that couples a biological sensing material associated with a transducer, which converts the information into a measurable effect, such as an electrical signal. It is used to detect a signal of an environmental change, either qualitatively or quantitatively. In 1962, Clark and Lyons developed the first enzyme based biosensor that is still widely used, which is the enzymatic amperometric glucose biosensor to determine the percent of glucose in the blood.[34] This measurement is done by measuring the gluconic acid and hydrogen peroxide that is produced due to the oxidation of β-D-glucose by oxygen that is catalyzed by glucose oxidase which is immobilized on the biosensor surface.[35] Biosensors have been used in many different applications such as the food industry, forensics, clinical diagnostics and environmental analysis.[36]

In the past two decades, considerable growth of interest in DNA biosensors can be attributed to their important analytical properties.[36] Most current DNA-based biosensors are based on DNA aptamers, and are referred to as aptasensors. DNA aptasensors exhibit excellent selectivity, high sensitivity, and can be used for the rapid detection of different viruses, bacteria, and various chemical substances.[37] DNA aptamers offer a number of advantages over traditional protein-based antibodies for rapid detection of disease biomarkers. Some of these advantages include desirable storage properties, such as excellent temperature and humidity stability, in addition, aptamers can be engineered and synthesized in test tubes without the need for animal systems, and are easily regenerated after denaturation, aptamers can be easily amplified via PCR, and they can be further modified with various functional groups.[21] Nowadays, aptasensors have the potential of being used as a highly sensitive diagnostic tool for many diseases. In the literature, Ban *et al.* developed an aptasensor for the detection of malaria which is an infectious disease caused by *Plasmodium* parasites.[38] In this example DNA aptamers for *Plasmodium* lactate dehydrogenase (pLDH) were prepared by SELEX using magnetic beads to bind to *Plasmodium vivax* LDH (PvLDH) and *Plasmodium falciparum* LDH (PfLDH). This interaction was measured by electrochemical impedance spectroscopy (EIS), which showed strong affinity between the aptamer and the protein. As a result, this aptasensor was used in a clinical environment to test blood samples from malaria patients. It showed promising results in detecting these two proteins at a low concentration of 1 pM. This aptasensor was also able to distinguish between malaria positive samples and non-infected samples.[38]

The most important aspect of the aptasensor, after choosing the right DNA aptamer as the probe molecule, is to ensure the immobilization of the probe on the surface of the electrode. Specific interactions will not occur between the probe and the target molecule if the probe is not immobilized with a certain orientation on the electrode. There have been several methods developed for the immobilization of DNA aptamers including physical and/or electrochemical adsorption, covalent attachment, and chemisorption.[35] The simplest method that is widely used is the covalent attachment which is fulfilled when the electrode contains certain metals such as gold or silver. In order for the DNA aptamer to bind to the metal it is modified with an n-alkanethiol $(X(CH_2)_n)$ SH either at the 5' or 3' end; this results in the formation of a strong metal-sulfur bond, while the short chain alkane reduces the likelihood of surface-induced denaturation of the DNA aptamer. In addition to the aptamer, regular alkanethiols are also added to the sensor surface and act as spacers. The role of these spacer thiols is to ensure that the DNA aptamer is immobilized vertically on the electrode surface, which makes it more accessible for hybridization. Spacer thiols cover empty spots on the electrode to prevent non-specific binding, and also helps in preventing surface-induced denaturation of the DNA aptamer.[39,40] A schematic of this sensor surface is shown in Figure 3.
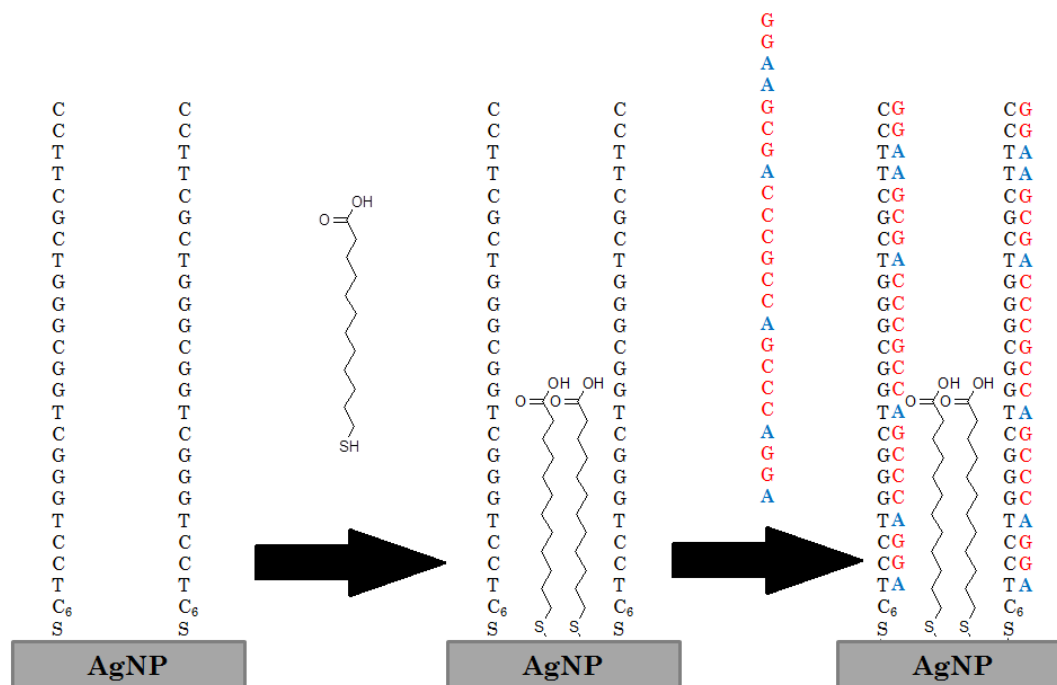
Figure 3: Illustration of the aptasensor surface with the DNA aptamer (probe) covalently attached to the AgNP electrode, and the addition of a thiol spacer, 12-mercaptododecanoic acid (12-MDA) to facilitate hybridization. The probe is shown in black, with its complementary strand (target) shown in red, and adenine shown in blue for emphasis.

1.2.5 IS6110 DNA Fragment

Biomarkers are biological markers that are associated with a biological state or used as an indication of a certain disease. There are some TB biomarkers that can be present in the patients' urine, blood and sputum samples. Examples of TB biomarkers include a peptide antigen (*6 kDa Early Secretory Antigen (ESAT6)*), a heme protein (*KatG catalase-peroxidase*), a large glycolipid (*Lipoarabinomannin (LAM)*) and DNA fragments (*IS6110 DNA fragments*), (For details, please refer to Figures A1-A4 in the Appendix section). The DNA fragment will be used as the biomarker for the detection of *M.tb.* for this study. These DNA fragments can be found in patients' urine, and are derived from cell-free nucleic acids that are present in plasma and blood. These cell-free

12

nucleic acids originate from the breakdown of DNA released from dead microorganisms.[41] These fragments usually pass through the kidneys, where they are then excreted into urine as trans-renal DNA (tr-DNA). Tr-DNA has been used to detect many chronic infectious diseases, more specifically tuberculosis, due to its accurate diagnostic power.[41] The genomes present in these fragments are similar to the ones found in bacteria, which consist of mobile genetic elements (MGEs).[42] These elements are capable of extracting themselves from one region of the genome and inserting themselves into another region.[42] These elements are found to contribute to DNA polymorphism in *M.Tb.* and are called insertion sequences (IS), of which IS6110 is an example.[6,42-44]

The IS6110 is related to the IS3 family, and is considered to be the most abundant IS found in the *MTBC* family.[43-45] This sequence is not randomly inserted into *M.Tb.* however; instead the sequence is inserted into "hot spot" regions which contain the Direct Repeats (DRs).[42,43] The DR region is present in all strains of *MTBC*, and it is characterized by multiple copies of a 36 base-pair sequences with unique inverting sequences between the DRs.[46] The IS6110 is used as a probe to hybridize specifically to a segment of the DNA fragment to identify specific strains present in the *M.Tb.* using a technique called restriction fragment length polymorphism (RFLP).[43,47-49] For this aptasensor, the IS6110 DNA fragment biomarker will be used as a target that would be detectable by binding to a specific probe molecule. However, basic studies should first be performed by using a DNA aptamer (probe) that would be immobilized on the SERS substrate, which would then bind to a sequence present in the IS6110 (target). The goal of this thesis work is to present proof of concept work towards the development of a

DNA aptasensor based on E-SERS that may demonstrate promise for the rapid detection of TB DNA fragments in patient urine at the POC.

1.3 Theory

1.3.1 Electrochemistry

Electrochemistry is a branch of chemistry that involves using electrical measurements to observe chemical effects. The chemical effects may consist of the movement of charged species that occur in bulk solution by using electrical quantities such as current, potential or charge. Electrochemistry has been widely used in many applications, such as environmental monitoring, industrial quality control, and biomedical analysis.[50] Potentiometric and potentiostatic methods are two types of measurement techniques used in electrochemistry. Both techniques use an electrochemical cell, which requires the presence of electrodes that are immersed in an electrolyte.[50] The electrolyte is an aqueous salt solution that conducts electricity, thereby allowing current to travel between the electrodes. The electrolyte used should not react with the analyte, it should have a concentration between 0.01-1.0 M, and it should not be reduced or oxidized easily. The presence of oxygen in the electrolyte solution can cause problems while doing electrochemistry. An easy way to remove oxygen is to purge the solution with an inert gas, such as argon or nitrogen, prior to use.[50]

A potentiostatic device known as a potentiostat is used in applying and controlling the potential across the cell. It has many advantages such as low cost, wide linear range, portability and high sensitivity.[50] In most cases, an electrochemical cell will contain three electrodes, which includes a reference electrode (RE), a counter electrode (CE), and a

working electrode (WE).[51] The RE has a constant potential that is not affected by the applied potential. The most commonly used ones are Ag/AgCl and Hg/Hg_2Cl_2 (standard calomel electrode).[50] A CE, such as a platinum wire, completes the cell circuit with the WE. The CE functions without interfering with the WE, by acting as an anode when the WE is acting as a cathode and *vice versa*.[52] The WE is where the reaction of interest takes place. One of the common working electrodes widely used in electroanalysis is carbon. Carbon WEs have a wide potential window, a low cost, they demonstrate chemical inertness, and have desirable mechanical and electrical properties.[50] One electrochemical method that is pivotal to this research project is that of cyclic voltammetry (CV), which is a good indicator for the presence of tethered layers of thiol terminated aptamers on the electrode. CV is a qualitative method that consists of linearly scanning the potential of the working electrode, and the potentiostat simultaneously measures the current resulting from the applied potential. A cyclic voltammogram is the resulting plot of the measured current versus the applied potential.[50] CV can be used prior to performing an electrochemical analysis since it indicates whether the electrode and electrolyte are clean. In addition, it can be used to determine whether or not a monolayer has formed on the surface. During application of an applied voltage, charged molecules will move closer to or away from the electrode surface depending on their charge. A negatively charged molecule will be attracted to a positively charged electrode, which causes the formation of a double layer. Applying a potential in the positive or negative direction can alter the charge of the WE surface which can attract oppositely charged molecules.[51]

1.3.2 Raman Spectroscopy

Raman spectroscopy is considered to be one of the commonly used vibrational spectroscopic methods that provides qualitative information about an analyte sample. This technique is based on the inelastic scattering of incident monochromatic excitation light. When source radiation is focused onto a sample, the photons can be scattered either elastically or inelastically by the sample.[53] Looking at Figure 4, there are three different types of light scattering that could occur, which are Rayleigh, anti-Stokes and Stokes scattering.[54] Rayleigh scattering, or elastic scattering, occurs most often. The excited molecule returns back to its ground state with no net energy transfer, and therefore elastically scattered light does not contain any vibrational information about the molecules present in the sample. Anti-Stokes Raman and Stokes Raman scattering occur when there is a net energy gain or loss, respectively, and both processes provide essentially identical vibrational information about the sample.[54] In most instances, molecules are present in their ground state, the Stokes Raman scattering effect is therefore stronger, and as such, it is used in almost all Raman spectrometers. Each molecule that is present in the sample will scatter light differently which will provide a unique spectral profile for each sample component.[53]

There are many advantages to using Raman spectroscopy as an analysis technique such as simplicity, small sample requirement, almost no sample preparation is required, it is non-destructive, and it offers rapid analysis time and portable instrumentation is widely available.[53,55,56] Another important reason for choosing Raman spectroscopy, as opposed to infrared spectroscopy (IR) for instance, is that Raman scattering is very weak for

water, carbon dioxide, alcohols and glass.[56] In general, the Raman effect is often very weak, since light is scattered inelastically in very small proportions. Usually one in one million photons undergo this type of scattering.[57] This inherent lack of sensitivity limited the widespread application of Raman spectroscopy, and it was mostly used on neat or powder samples between the time of discovery in 1928 until the 1970's when lasers became widely used light sources.[53,57]
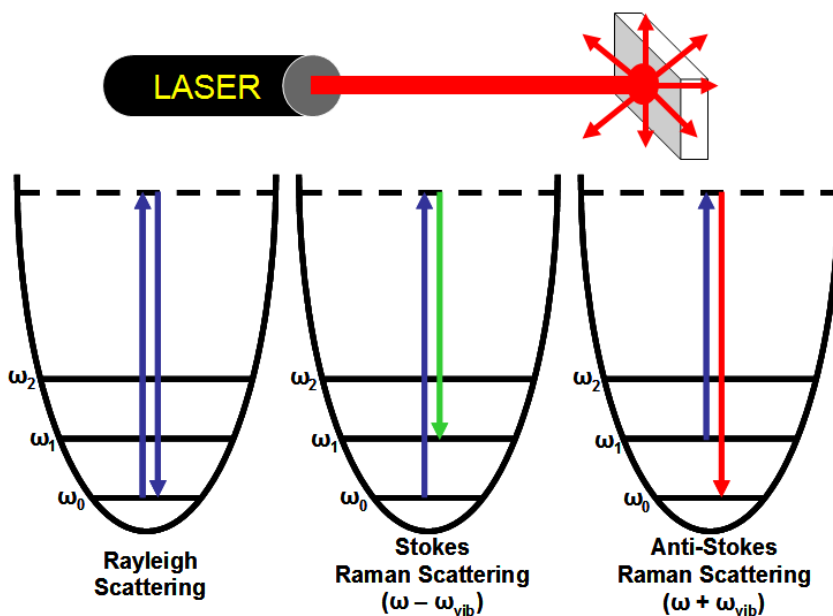
Figure 4: Diagram showing the different light scattering modes: Rayleigh, Stokes, and anti-Stokes scattering.

1.3.3 Surface-Enhanced Raman Spectroscopy (SERS)

In 1974, research done by Fleischmann *et al.* showed that pyridine and other molecules exhibit an enhancement in their Raman signal when adsorbed onto an electrochemically roughened silver surface.[58] After this observation, Van Duyne and Jeanmaire examined some factors that would affect the intensity of the Raman signal, such as surface roughness and applied potential of the electrode, solution analyte

17

concentration, and electrolyte composition of the solution.[59] This analysis led to the great discovery that molecules present on the surface of a nanostructured coinage metal surface (most commonly Ag, Au and Cu) can exhibit an extraordinary enhancement in their Raman signal (Figure 5).[60] This phenomenon is referred to as Surface-enhanced Raman spectroscopy (SERS) which is a very selective and sensitive technique that increases the magnitude of the Raman signal of an analyte by 10^4 to 10^{11} orders of magnitude.[57] The mechanism leading to this enhancement is not completely understood.[61] However, it is believed that this enhancement is due to both electromagnetic and chemical enhancement mechanisms.[57,62] The electromagnetic contribution is a wavelength-dependent effect that contributes up to 10^{12} orders of magnitude in terms of signal. This effect arises from the collective oscillation of conduction electrons that occurs when an electromagnetic wave (i.e. incident radiation of a laser) interacts with a metal surface.[62,63] This interaction results in a strong electromagnetic field that is caused by the localized surface plasmon resonance (LSPR) due to nanoscale features of the metal surface. The LSPR is dependent on the size, shape, nanometric roughness, and the material of the nanostructured surface.[57,63] The chemical effect contributes up to 10^2 orders of magnitude to the enhancement, and is due to charge transfer between the molecule and the metal surface. This chemical mechanism can vary between substrates, adsorbed molecules, and substrate adsorption sites.[57]
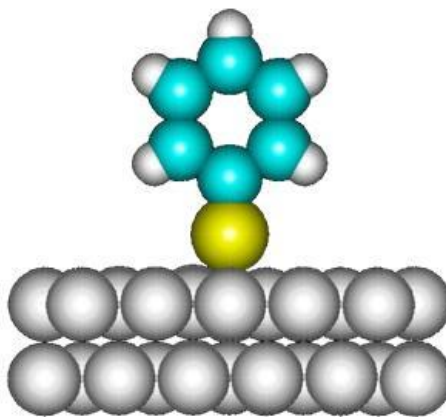
Figure 5: Benzenethiol chemically adsorbed onto a metal nanoparticle surface. (not drawn to scale)

This technique can be coupled with electrochemistry (E-SERS) to detect the signal of the analyte present on the metal surface at a chosen applied voltage. Electrochemical SERS can be useful in detecting the signal of the analyte in a relevant biological environment, to observe how the molecules change conformation or orientation at different applied voltages, and also to observe the electrochemical stability of certain analytes. Nanoparticles have been increasingly used in analytical chemistry because they exhibit unique chemical, physical, optical and electronic properties due to their small size, which ranges from a few to a few hundred nm in diameter.[64] There has been an increasing demand in using these nanoscale materials in many technological applications instead of using bulk materials. Lately, nanoparticles have been used in a variety of different fields such as chemistry, biology, physics, medicine, materials science, engineering and computer science.[65] There are many types of metal nanoparticles being used in SERS; however, the two most common metals are gold and silver. Silver nanoparticles (AgNP) are often preferred because they give excellent SERS enhancement, they are relatively stable and inexpensive to make, and they function as a

stable electrode material. There are many methods being used to prepare these metal nanoparticles; however, some of these methods, while providing interesting nano-structures, result in nanoparticles which are not SERS-active. The Lee-Meisel method is most often used to form colloidal silver nanoparticles via citrate reduction of silver which demonstrates excellent SERS activity.[66]

A common problem that one can face when using SERS for the detection of DNA is that the SERS technique is highly distant dependent. The LSPR that is generated is localized on the surface, and hence the decay length is very short. As a result, the analyte being tested should be within a certain range of the surface of these silver nanoparticles for it to experience the signal enhancement. According to the literature, the ideal distance for SERS detection is within 2-4 nm of the nanoscale roughness features.[57] The SERS intensity of certain analytes present on the metallic surface also depends on the orientations of these molecules and the tensor symmetry with respect to the surface. The concept of surface selection rules (SSRs) was developed by Moskovits[67], which discusses the local field polarizations of the molecule and its connection with increasing the observed SERS intensity. The SSR suggest that the local field polarization should be perpendicular to the SERS substrate to give rise to higher SERS intensity, while on the other hand, if it is parallel to the SERS substrate the signal will be weaker.[68]

1.3.4 SERS-Based Sensing

SERS has been used in many different fields including chemistry, biology, geology, materials science, electrochemistry and surface science. SERS has been widely used for sensing materials because it offers several advantages over other sensing

methods. SERS has the ability to be used for single molecule detection, making it one of the most sensitive analytical methods available. In addition, since SERS is based on vibrational spectroscopy, it has molecular fingerprinting capability.[61] One of the limitations of using SERS in sensing is that SERS substrates are not very reproducible, which can reduce the sensitivity and make quantitative analysis problematic.[57] In the literature, there are numerous examples of research focusing on using SERS for sensing. For example, SERS has been used to detect a variety of molecules, including melamine[55], glucose[69], and uric acid.[70] Recently, aptamers and SERS have been combined as an even more powerful sensing tool. An example is Yu *et al*., who looked at using SERS for developing an aptameric sensor for the rapid detection of cocaine.[71] This study was done by measuring the change in signal that would result from binding the cocaine molecule to an aptamer that contains tetramethylrhodamine (TMR) as a Raman reporter label. Upon binding, the aptamer changed conformation, which brings the TMR molecule into close proximity to the SERS surface leading to an increase in the SERS signal. In order to control the folding of the aptamer and mitigate steric hindrance during conformational changes, 3-mercaptopropionic acid (3-MPA) was used as a spacer molecule. The aptamer and 3-MPA were immobilized on the surface of the SERS substrate, which consisted of a silver colloid film on a polished gold disc.[71] The results obtained for the detection of cocaine were very successful, and show promise for the use of this technique as opposed to fluorescence and electrochemical sensors. It was reported that the concentration of cocaine that could be measured in the range from 1 to 3200 µM under optimized assay conditions. This SERS-based aptamer sensor provides quick analysis, it is easy to use, and it can be reused after a simple wash.[71] This example is one of many in the literature

which show how SERS has been widely used for sensing.

As seen in the literature, a point-of-care device is needed for the rapid detection of tuberculosis biomarkers. In this project, this will be achieved using specific DNA aptamers that will be immobilized on the AgNP electrodes, which will function as a probe for detecting TB biomarkers. E-SERS will be used to detect any change in signal due to the binding occurring between the probe and the biomarker.

Chapter 2: Results and Discussion:

2.1 DNA Base Studies

2.1.1 Normal Raman

In order to begin studies on DNA aptamers using E-SERS, initial studies were done on the four DNA bases individually. These studies are helpful for the interpretation of the whole DNA aptamer. The first study investigated the normal Raman signal for the pure powder of each base. This was done by placing a small amount of the powder on a glass slide and directing the laser of the Raman spectrometer onto it. As shown in Figure 6, each DNA base gave a unique spectral profile. Each base showed a strong peak in the range between 600 and 800 cm^{-1} which is indicative of a ring breathing vibration.[72] There are some strong peaks that can be used to distinguish these bases from each other; for example, guanine (650, 1266 cm^{-1}), adenine (723, 1334 cm^{-1}) cytosine (790, 1278 cm^{-1}), and thymine (1371, 1673 cm^{-1}). These results were used to build a reference library for the DNA bases; all the peaks and their corresponding assignments are listed in Tables A-1 to A-4 in the Appendix section.
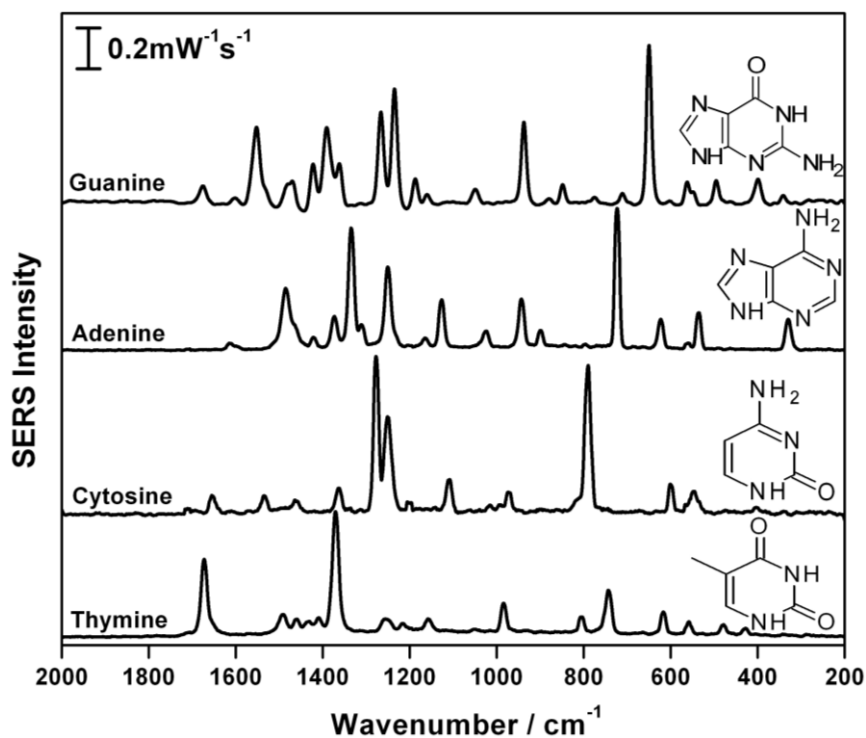
Figure 6: Normal Raman spectra for the four DNA bases: guanine, adenine, cytosine and thymine. All spectra were collected at medium power (22.3 mW) for a time interval of 30 seconds.

2.1.2 E-SERS

Due to the inherent lack of sensitivity with normal Raman spectroscopy, the previous measurements were done on pure powders, which is not generally very useful for detection of analytes in solution at low concentration. Since normal Raman spectroscopy has poor sensitivity and it will not be able to detect these DNA bases at low concentration, SERS was used to measure these analytes instead. Solutions of DNA bases with a concentration of 1.0 mM were thus prepared in 0.1 M NaF as supporting electrolyte which was used for the SERS studies. In particular, E-SERS was used to help characterize the behavior of the DNA bases at the metal/solution interface. By looking at Figure 7, it is apparent that the adenine signal increases ~10-fold simply by changing the

24

voltage. This effect is most likely due to a change in the surface chemistry/charge of the AgNP electrode, which occurs due to the application of a negative voltage. Open circuit potential (OCP) is the resting potential for the metal and it is measured without applying any potential. At OCP, the surface of the AgNP electrode is negatively charged due to the adsorbed citrate present. Therefore, by applying a negative voltage the citrate is desorbed, which allows the adenine to bind more strongly to the surface. Similar results were also obtained for the three other bases (data not shown). These results indicate that a stronger SERS signal of the DNA bases can be obtained by applying a negative potential.
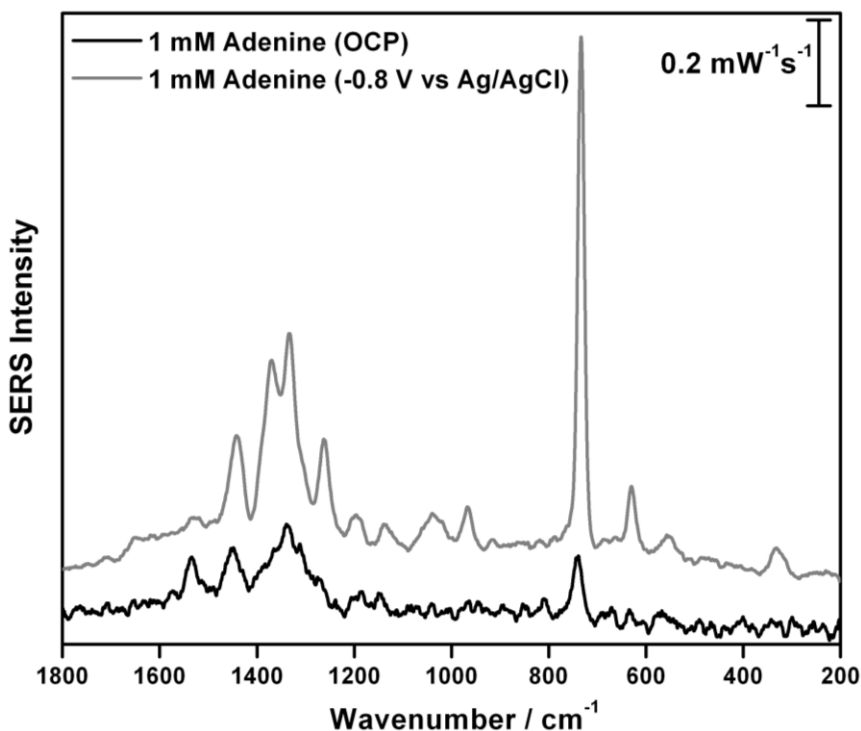
Figure 7: SERS signal of 1.0 mM adenine at OCP (black curve), and at -0.8V (grey curve). At OCP, the signal was collected at medium-high power (46.5 mW) for a time interval of 20 seconds, and at -0.8 V, it was collected at the same power for a time interval of 60 seconds.

2.2 DNA Nucleotide Studies

2.2.1 Normal Raman

Nucleotides are basically DNA bases connected to a ribose sugar group and a phosphate group, as shown in Figure 8. The four DNA nucleotides used in this research were 2'-deoxyadenosine 5'-monophosphate (dAMP), 2'-deoxycytidine 5'-monophosphate (dCMP), thymidine 5'-monophosphate (dTMP), and 2'-deoxyguanosine 5'-monophosphate (dGMP). Normal Raman spectroscopy of the four DNA nucleotides was performed in the same way as was discussed previously in the DNA base study section. By looking at Figure 9, it is apparent that a Raman signal for the DNA nucleotide was obtained. However, the signal collected was weaker than the one collected for the base itself. The peaks observed were not as intense, and the signal-to-noise ratio was low, especially in the case of the purines. According to the literature, nucleotides have weak Raman signals because the sugar and phosphate groups are weak Raman scatterers, essentially diluting the observed signal.[73]
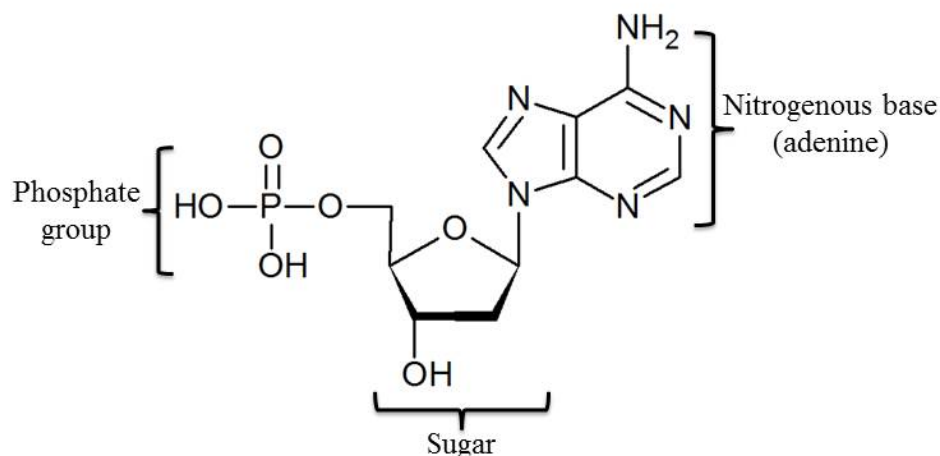
Figure 8: DNA nucleotides consist of a nitrogenous base, sugar, and phosphate group. In this case adenine represents one of the four nitrogenous bases.

26
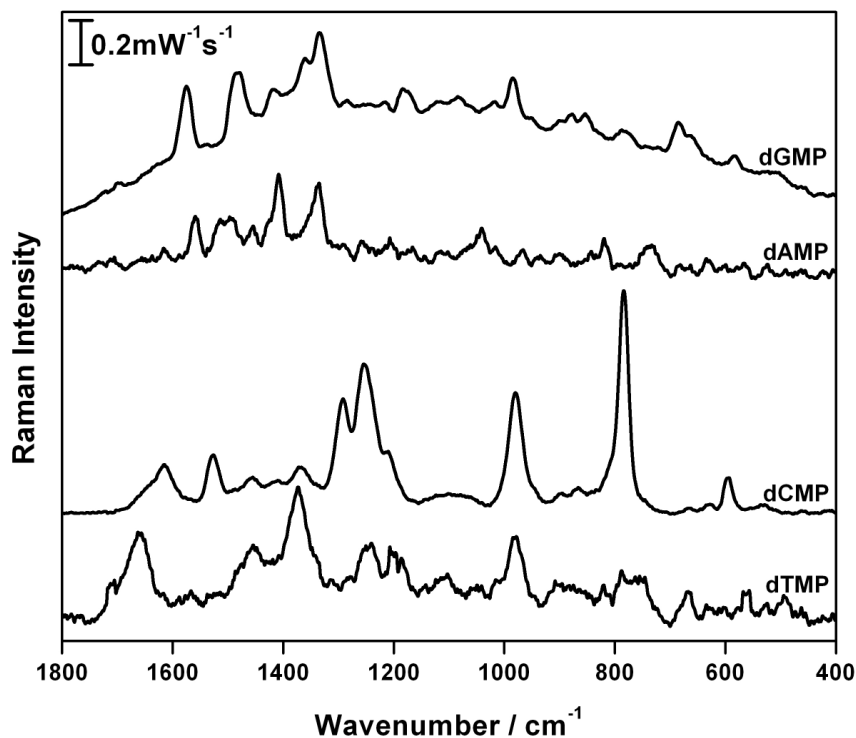
Figure 9: Normal Raman spectra for the four DNA nucleotides: dGMP, dAMP, dCMP, and dTMP. Adenine was measured at medium-high power (46.5 mW) for a time interval of 60 seconds, while the rest were measured at high power (55.9 mW) for a time interval of 60 seconds.

2.2.2 E-SERS

The studies presented previously showed very promising results for using Raman spectroscopy, and more specifically E-SERS for the detection of DNA bases. However, DNA aptamer sequences contain nucleotides and not simply the DNA bases. By performing E-SERS on these nucleotide solutions, it was observed that the SERS signal can be observed at negative applied voltages, and it is indeed dominated mostly by the DNA base. This is illustrated in Figure 10 using adenine as an example.
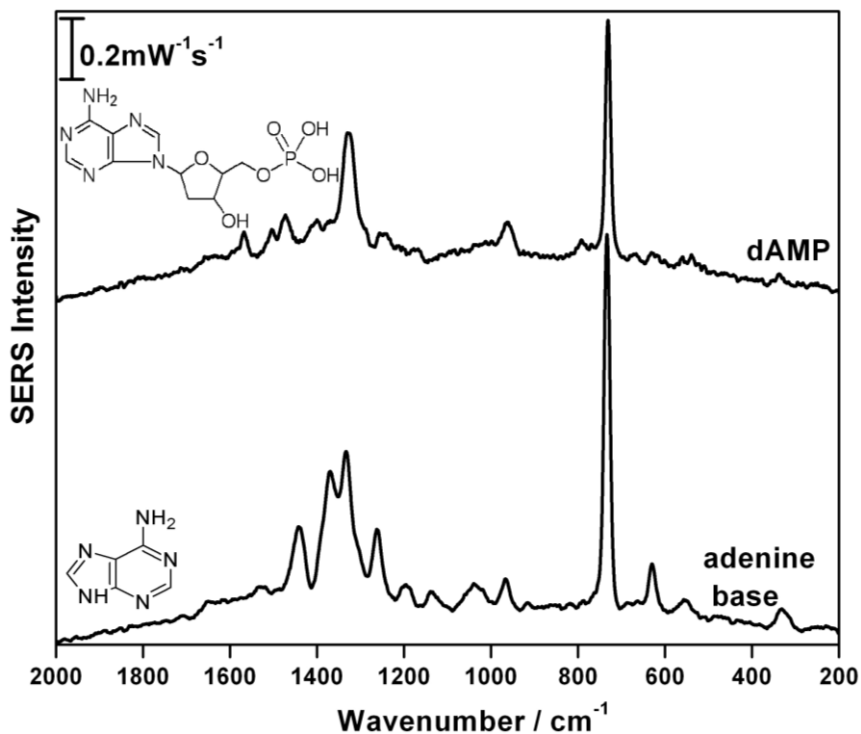
Figure 10: Comparison between the adenine base and dAMP at -0.8V using E-SERS. Both spectra were collected at medium-high power (46.5 mW) for a time interval of 60 seconds.

E-SERS was performed on the other three nucleotides and similar results were obtained; each nucleotide gave a unique spectral profile as well, with the dominant features coming from the base in each case (data not shown). In the literature, it was mentioned that dAMP might dominate the signal over the other nucleotides when present in a mixture.[73] This issue could be problematic in the development of a SERS-based DNA sensor. To test this theory, E-SERS was performed in a solution containing all four nucleotides with the same concentration of 1.0 mM. By looking at the overlaid spectra of the nucleotides in Figure 11, it is shown that the signal was not dominated by any one nucleotide. An equimolar mixture of all four nucleotides was prepared, and is also shown in Figure 11. By comparing the mixture solution spectrum with the nucleotide spectra, it

can be seen that there were some peaks present that are indicative of each of the nucleotides present. For example, adenine (732, 1328 cm^{-1}), guanine (683, 1481 cm^{-1}), cytosine (789, 1636 cm^{-1}), and thymine (792, 1650 cm^{-1}). These peaks are different than the ones recorded for the DNA bases themselves, due to presence of the sugar and phosphate moieties. By these studies, it was concluded that E-SERS will be able to detect the nucleotides in a DNA aptamer, and the signal most likely will not be dominated by any particular nucleotide.
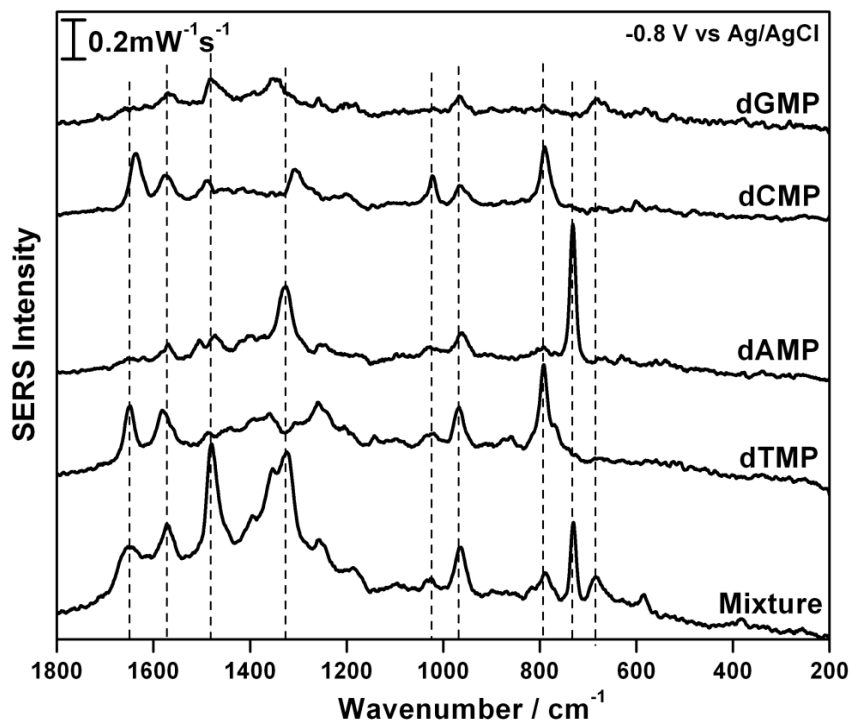
Figure 11: E-SERS comparison of the four nucleotides, as well as the mixture of bases, at -0.8V. All the spectra were collected at medium-high power (46.5 mW) for a time interval of 60 seconds.

2.3 DNA Aptamer Studies

2.3.1 Probe 1 Studies

The first DNA aptamer investigated, henceforth referred to as probe 1 (P_1), was a small DNA fragment containing 23 nucleotides, as shown in Table A-5 in the Appendix section. This sequence was specifically engineered to not contain any adenines, which would help in detection of hybridization with its complimentary strand, referred to as target 1 (T_1), which does contain adenine, and will thus be a proof of concept for hybridization studies of the target biomarkers, as will be shown later. The sequence of this DNA aptamer (probe 1) was modified to have a thiolated 5' end as well as a six carbon spacer. The thiolated end ensures a strong attachment to the AgNP electrode, while the six carbon spacer helps prevent surface denaturation of the DNA. The disulfide bond (S-S) is usually reduced at noble metal surfaces to form a thiol when the DNA aptamer chemically adsorbs onto the AgNP surface, which can be confirmed by not observing a υ(S-S) peak around 542 cm^{-1}.[74] Figure 12 shows the E-SERS cathodic signal of P_1 deposited on the AgNP electrode. At OCP the signal was mostly due to the citrate present on the AgNP; citrate usually has apparent peaks at ~1390 and ~933 cm^{-1} which are assigned to υ_s(COO) and υ(C-COO) respectively.[75] As the voltage was decreased, the citrate signal decreased because the surface charge of the metal became less positive, which then repels the negatively charged citrate from the surface. At -0.5 V some peaks appeared, which are due to P_1, and the signal was observed to increase as the potential was made more negative. At -1.0 V, the signal is a result of the probe only, and the citrate signal is no longer present. For example, peaks around 790, 1257 and 1577 cm^{-1} are due to cytosine, thymine, and guanine, respectively.[53] The peak at ~687 cm^{-1} is

30

indicative of the C-S stretch,[27,76] suggesting that the aptamer has indeed formed a self-assembled monolayer (SAM) on the AgNP surface. All of the peaks and corresponding assignments are listed in Table A-6 in the Appendix section.

Figure 12: E-SERS cathodic signal of P_1 immobilized on a AgNP electrode, measured at medium-high power (46.5 mW) for a time interval of 60 seconds.

After applying a negative voltage up to -1.0 V, the voltage was then stepped back in the anodic direction to 0.0 V to determine whether or not this monolayer would be stable. It will also show if there would be any change of confirmation of the aptamer by applying a more positive voltage. The probe signal increased slightly as the potential was made less negative, as is shown in Figure 13. This observation is indicative that the confirmations of these nucleotides are changing slightly on the surface of the AgNP electrode as potential is applied, and furthermore that the probe is strongly adsorbed. If the signal is increasing in intensity, there are several possible explanations, such as the

nucleotides moving closer to the SERS substrate, or the conformation could be changing such that the polarizability tensors are directed along the surface normal.

Figure 13: E-SERS anodic signal of P_1 immobilized on a AgNP electrode, measured at medium-high power (46.5 mW) for a time interval of 60 seconds.

In most cases, after performing E-SERS on the surface of the WE, CV is then performed to test if the electrode is functioning properly. The results can also act as a proof for the presence of a SAM on the WE. The swept potential is applied in cycles either once, or many times, depending on the information needed. Most of the CVs conducted in this research work were collected for 10 cycles because the first few cycles might not be stable. In Figure 12 and Figure 13, the E-SERS results obtained showed that P_1 was present on the surface of the WE. Consistent with this observation, if a stable SAM is indeed formed, the cyclic voltammogram will appear narrower in current. Figure 14 represents CV results obtained for a bare AgNP electrode and for an electrode

containing P_1 both measured in NaF electrolyte solution. It is apparent that the CV for the AgNP electrode containing a SAM did indeed appear narrower than the bare electrode, which indicates that the P_1 was immobilized on the electrode surface.
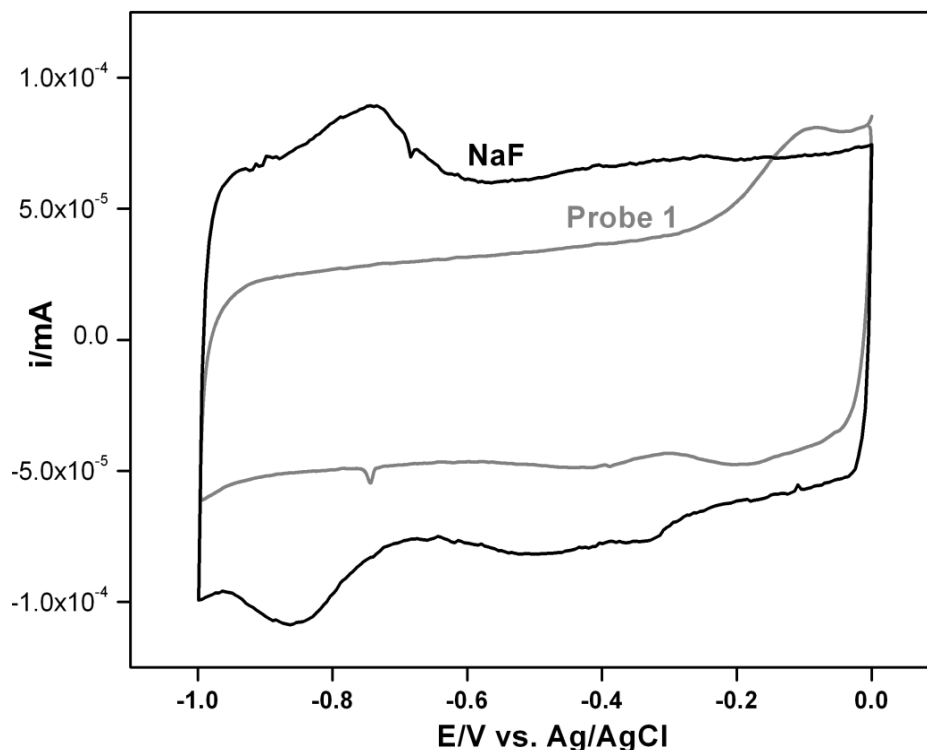
Figure 14: Comparison between the cyclic voltammogram of a bare electrode in NaF (black curve) and electrode containing a monolayer of P_1 (grey curve). Scan rate 50 mV/s. Potential ranged from 0.0 to -1.0 V vs. Ag/AgCl.

2.3.2 Target 1 Studies

A problem that might arise with these DNA aptamer surfaces is non-specific binding onto the SERS substrate by non-target analytes, such as non-target DNA. Surface-induced denaturation of the aptamer might also be an issue, since the DNA aptamer could be adsorbed horizontally onto the surface, and not vertically through the thiolated end. If it were to happen in this manner, the aptamer will not be able to bind properly to the target analyte. In order to test the extent to which non-thiolated DNA

binds to AgNP surfaces, E-SERS was done on the complementary strand for probe 1, referred to as target 1. This sequence has the same number of nucleotides as P_1, however, it is not thiolated and it contains adenine, as shown in Table A-5 in the Appendix section. In theory, since this sequence is not thiolated, it should not adsorb strongly onto the surface, and therefore no signal should be detected. Figure 15 shows that even without applying any voltage (i.e. measuring only at OCP) the signal is strong for this DNA sequence. This result proves that non-specific interactions between non-thiolated DNA fragments and the SERS substrate will most likely occur. The peaks that are present are due primarily to the adenine (730, 1328 cm^{-1}), which indicates that adenine might indeed dominate the signal and that most of the surface interactions may be driven by this moiety. As the potential was decreased, the intensity of the adenine signal was observed to become stronger. This non-thiolated interaction is likely occurring between the nitrogens present in the exposed nucleotides and the AgNPs.
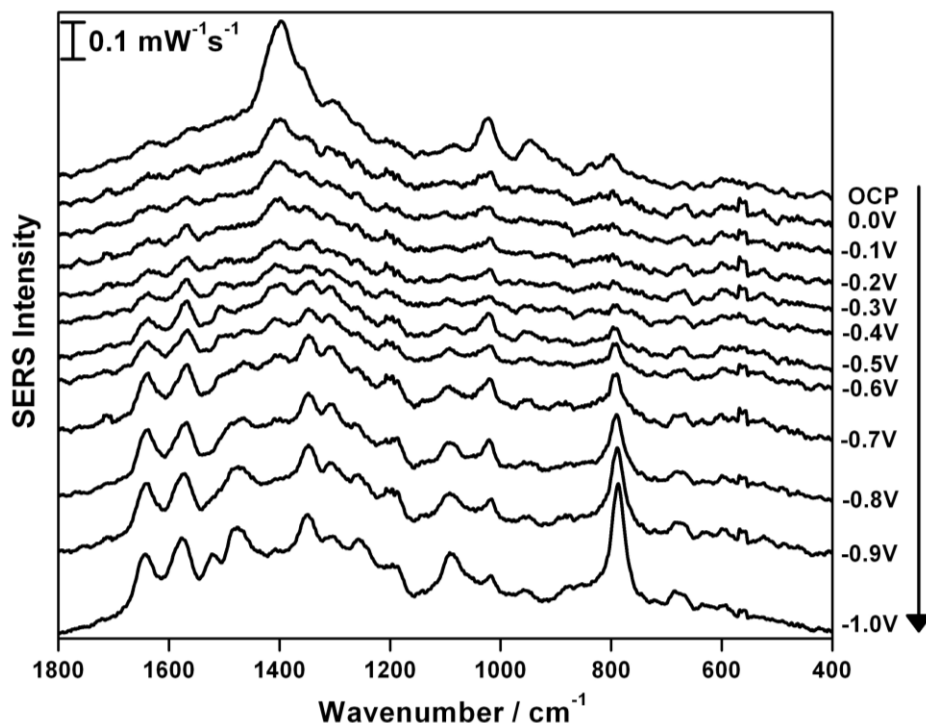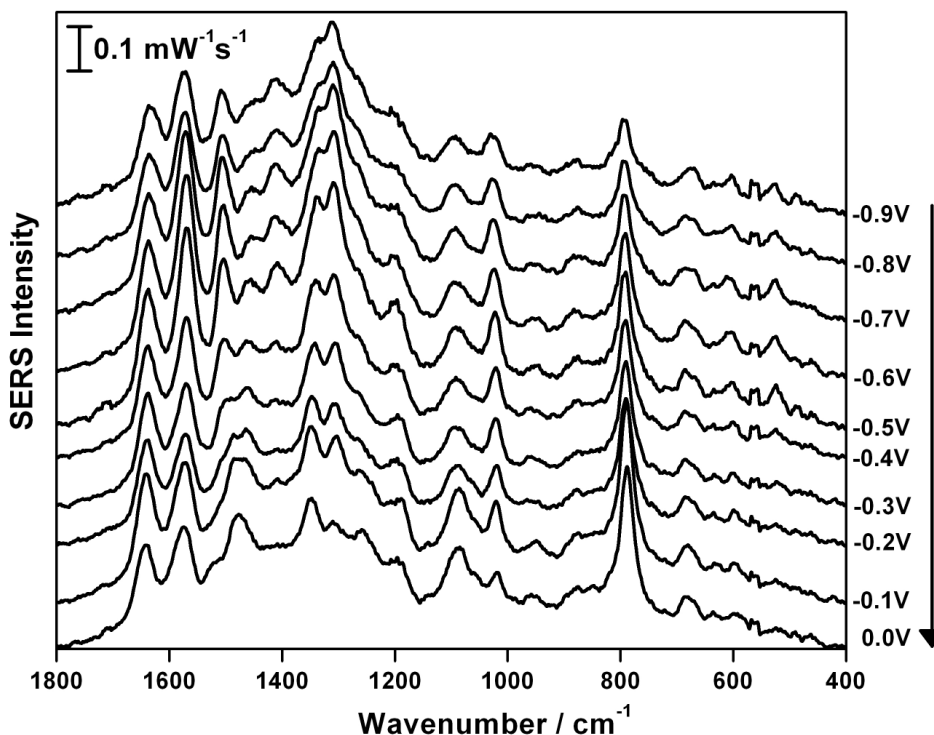
Figure 15: E-SERS cathodic signal of T_1 immobilized on a AgNP electrode, measured at medium-high power (46.5 mW) for a time interval of 60 seconds.

2.3.3 Hybridization Studies: Probe 1 + Target 1

Since a signal was detected separately for P_1 and T_1, a hybridization study was then performed as a proof of concept experiment to show that the target TB DNA will have specific binding with the probe. These studies were done by immobilizing the probe on the SERS substrate, and then introducing the complementary strand which would then bind to the probe through base-pairing between the DNA bases. These results are shown in Figure 16; the appearance of peaks around 1330 and 730 cm^{-1} is indicative of the presence of adenine which is only present in the target DNA sequence. As such, it suggests that hybridization has indeed taken place.

Figure 16: E-SERS cathodic signal of hybridization study between P_1 and T_1 immobilized on a AgNP electrode, measured at medium-high power (46.5 mW) for a time interval of 60 seconds. Arrows indicate peaks due to adenine.

2.4 DNA Aptamer Control Study (Scrambled Target 1 "s.T_1")

2.4.1 Characterization of Scrambled Target 1 using E-SERS

Since non-specific binding occurred between T_1 and the SERS substrate, it cannot be assumed that the hybridization study indeed worked properly. The adenine peak was clearly present, (Figure 16) but it could be due to surface adsorption of T_1 and not from direct hybridization to the probe. A control study was done to examine this issue by using a DNA aptamer that is not the complementary strand for P_1. This DNA sequence is a scrambled sequence of target 1 (referred to as s.T_1), which means it has the same number of nucleotides, including the same number of adenines, but the sequence is scrambled such that the nucleotides will not be able to base-pair with P_1. The sequence

36

for s.T_1 is shown in Table A-5 in the Appendix section. E-SERS was performed on s.T_1 by itself before conducting the hybridization study. Figure 16 shows that the signal of this DNA sequence is apparent without application of any voltage. However, as the voltage was decreased, the signal increased, and more peaks were observed. The adenine peak (732 cm^{-1}) also increased in intensity; however the cytosine peak (785 cm^{-1}) was observed to be stronger.
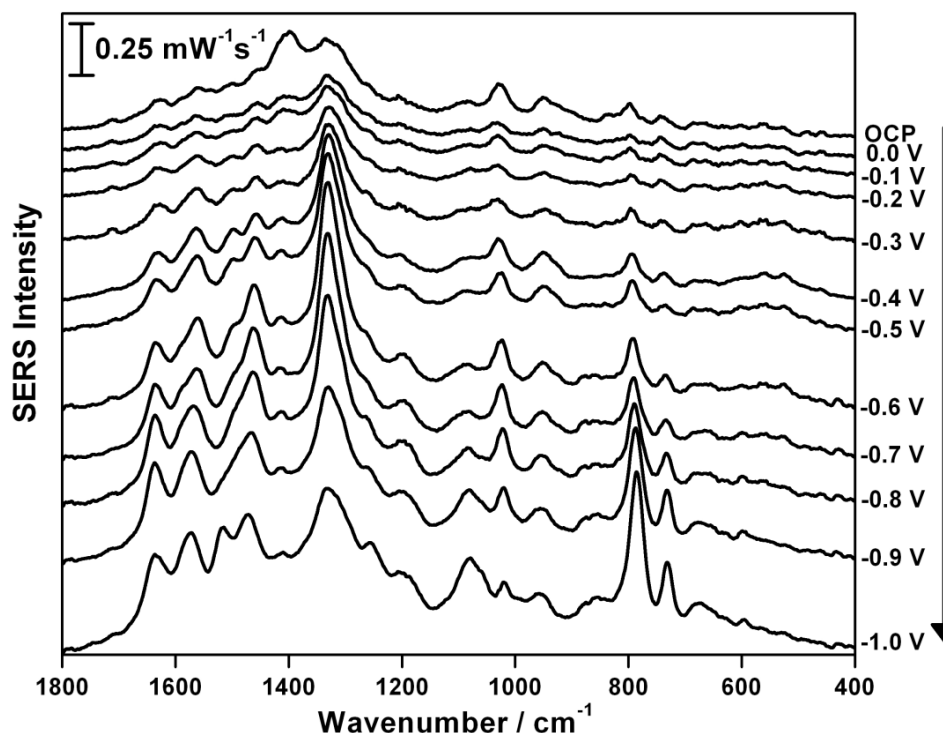
Figure 17: E-SERS cathodic signal of scrambled sequence of T_1 immobilized on a AgNP electrode, measured at medium-high power (46.5 mW) for a time interval of 60 seconds.

2.4.2 Hybridization Study Probe 1 + Scrambled Target 1

A hybridization study between P_1 and s.T_1 was performed in the same way as with T_1 (section 2.3.3). Figure 18 shows the results for this hybridization study, and by looking at the OCP spectrum before applying any voltage, the adenine peak (730 cm^{-1})

was already present. In the anodic signal, the adenine peak was also still present, and the signal was stable up to 0.0 V. This finding strongly suggests that a non-specific interaction between the s.T$_1$ and the SERS substrate is occurring, and not hybridization specifically. The s.T$_1$ was able to adsorb directly onto the AgNP surface. Such non-specific binding will cause false-positive hybridization results if the biosensor device is to be used in this manner in a clinical setting. Therefore, in order to reduce this non-specific binding, thiol-backfilling was explored. In thiol-backfilling, a thiol is added to the surface after the self-assembly of the aptamer to fill in any unoccupied surface sites, thus blocking access to the surface by non-specific adsorbates, including non-target DNA.
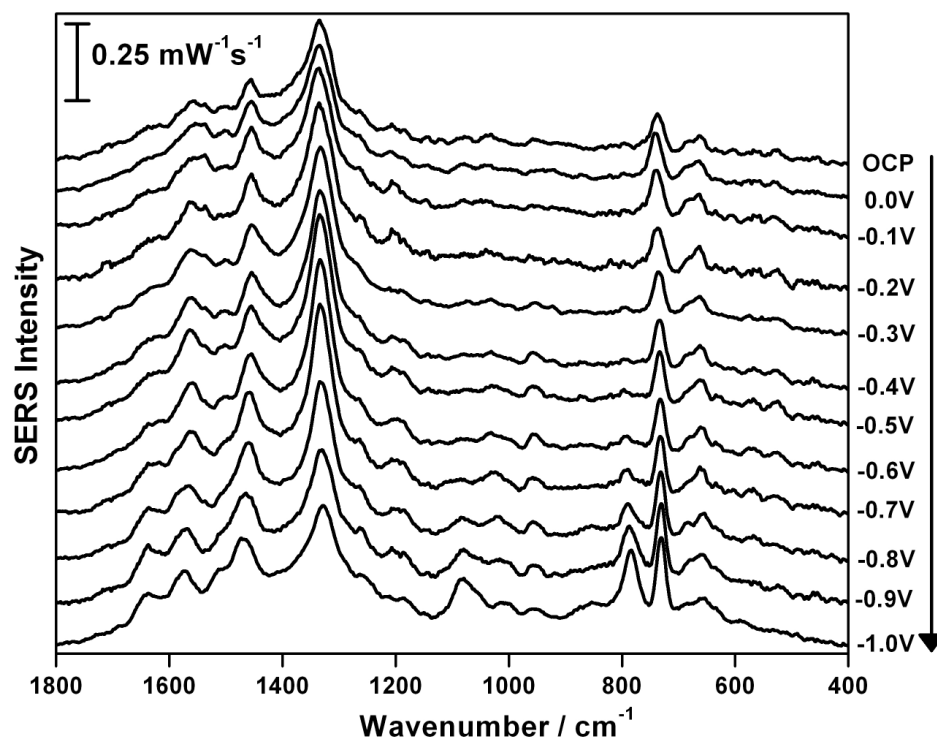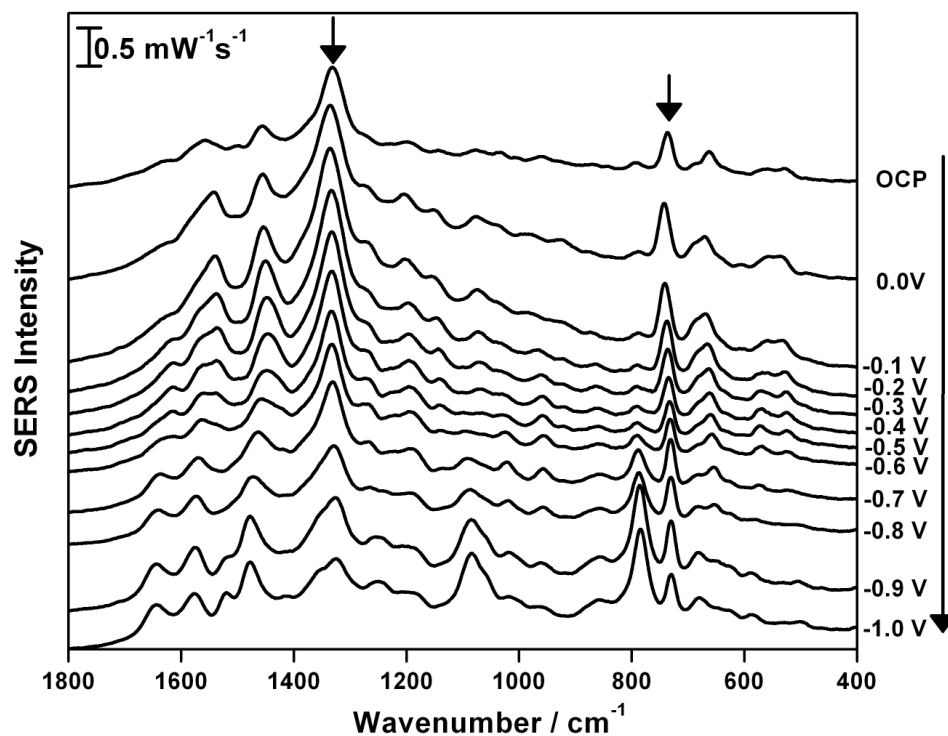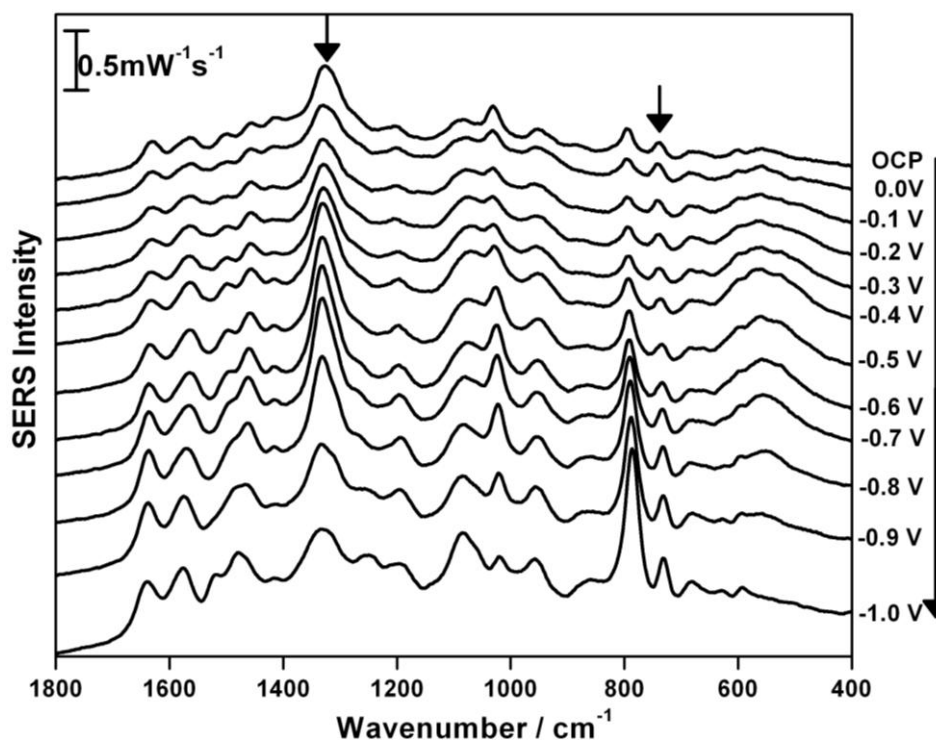

Figure 18: E-SERS cathodic signal for a hybridization study between P$_1$ and s.T$_1$ immobilized on a AgNP electrode, measured at medium-high power (46.5 mW) for a time interval of 60 seconds. Adenine peaks are indicated by arrows.

2.5 Characterization of Self-Assembled Monolayer (SAM) of Potential Spacer Molecules.

2.5.1 12-mercaptododecanoic Acid (12-MDA) Study

In order to try and prevent non-specific binding of the target, thiol-backfilling was explored. In thiol-backfilling, the SERS substrate, or electrode in this case, is incubated first in a solution of the aptamer, and then in a solution containing a thiol, typically an alkanethiol. The alkanethiol then takes up all available free surface sites, thus preventing non-specific adsorption onto the substrate. This alkanethiol is sometimes referred to as a spacer molecule. In order to choose a good thiol that would displace the citrate on the surface of the silver nanoparticles and act as a stable SAM, several thiols were tested including 6-mercaptohexanoic acid, 6-mercapto-1-hexanol, and 12-mercaptododecanoic acid (12-MDA). The first two thiols were not able to completely displace the citrate even after 24 hours of incubation. However, the 12-MDA was able to displace the citrate signal with only 2 hours of incubation as shown in Figure 19. The signal at OCP showed no citrate peaks at all, and the 12-MDA signal was very strong. The signal increased as the potential became more negative, and then it started decreasing around -0.7 V. The signal started increasing as the potential was going back positive direction (-1.0 V to 0.0 V), and the signal was mostly stable (data not shown). The peaks around 704, 1100, and 1435 cm^{-1} are indicative of CH_2 rocking, C-C vibrations, CH_2 scissoring, respectively.[77] The rest of the peaks and corresponding assignments are listed in Table A-7 in the Appendix section
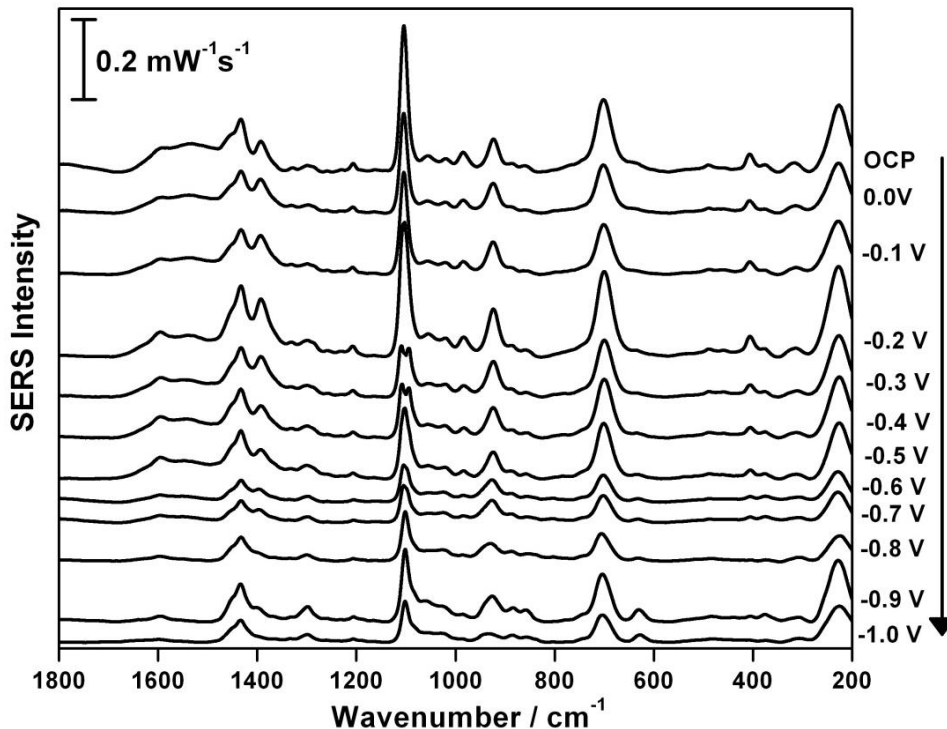
Figure 19: E-SERS cathodic signal of a AgNP electrode incubated in 1.0 mM of 12-MDA solution for 2 hours. The signal was measured at 120 mW for a time interval of 60 seconds using the 780 nm high resolution DXR Raman spectrometer.

2.5.2 Time Dependent Study of 12-MDA

An important aspect of choosing the correct thiol to act as a spacer for this project was to make sure that the thiol did not degrade over time, and neither displaced nor obscured the aptamer signal. In order to test its stability, the same electrode was tested several times over a period of time. The electrode was tested using E-SERS, followed by subsequent analyses after 68, 192 and 227 days as shown in Figure 20. It was observed that the 12-MDA signal was very stable on the SERS substrate over a period of time; all the peaks that were observed on the first day were still present and with similar intensity. After performing these tests, it was concluded that 12-mercaptododecanoic acid (12-MDA) would be used as the backfilling agent in the present study. By having the 12-

40

MDA present on the surface, non-specific binding should be eliminated, or at least, reduced significantly.
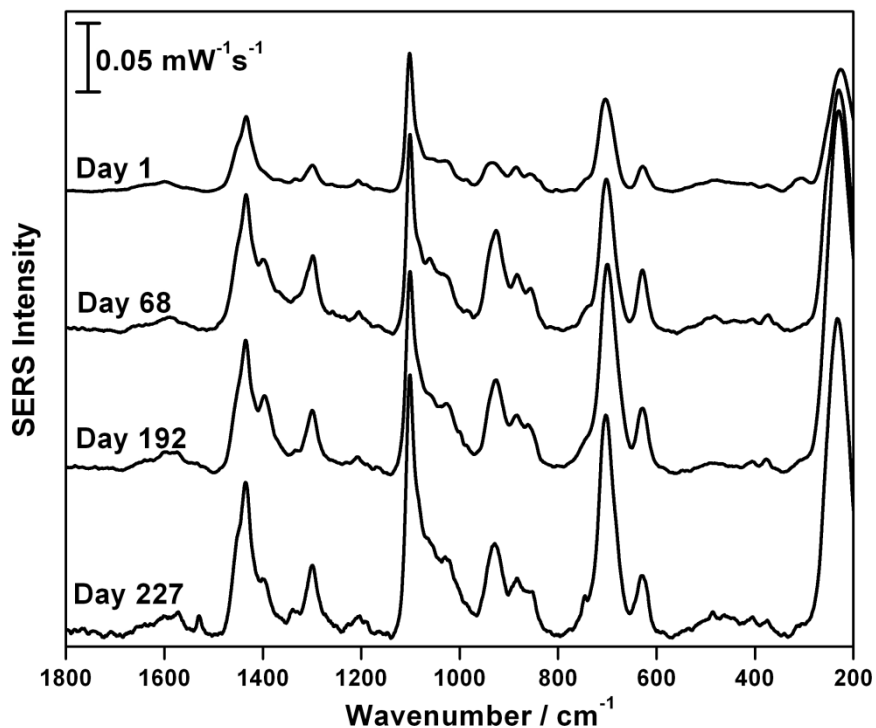
Figure 20: SERS signal collected at -1.0 V cathodic for a AgNP electrode initially incubated in 1.0 mM 12-MDA for 2 hours. All spectra were measured at the same parameters, 120 mW for a time interval of 60 seconds using the 780 nm high resolution DXR Raman spectrometer.

2.6 Hybridization Studies + Thiol-backfilling with 12-MDA Spacer

2.6.1 Probe 1 + Target 1 +12-MDA

For this study, the probe was first introduced onto the SERS substrate, and then the AgNP electrode was immersed in the 12-MDA solution. Next, the target aptamer was introduced for the hybridization study, as shown in Figure 3. Figure 21 shows the results obtained from this experiment. It was shown that the adenine peaks were already present at OCP. As the voltage was made more negative, the aptamer signal increased, as well as the adenine peaks. It shows that the 12-MDA did not displace the probe that was already

41

immobilized on the surface, and that hybridization could be directly monitored.
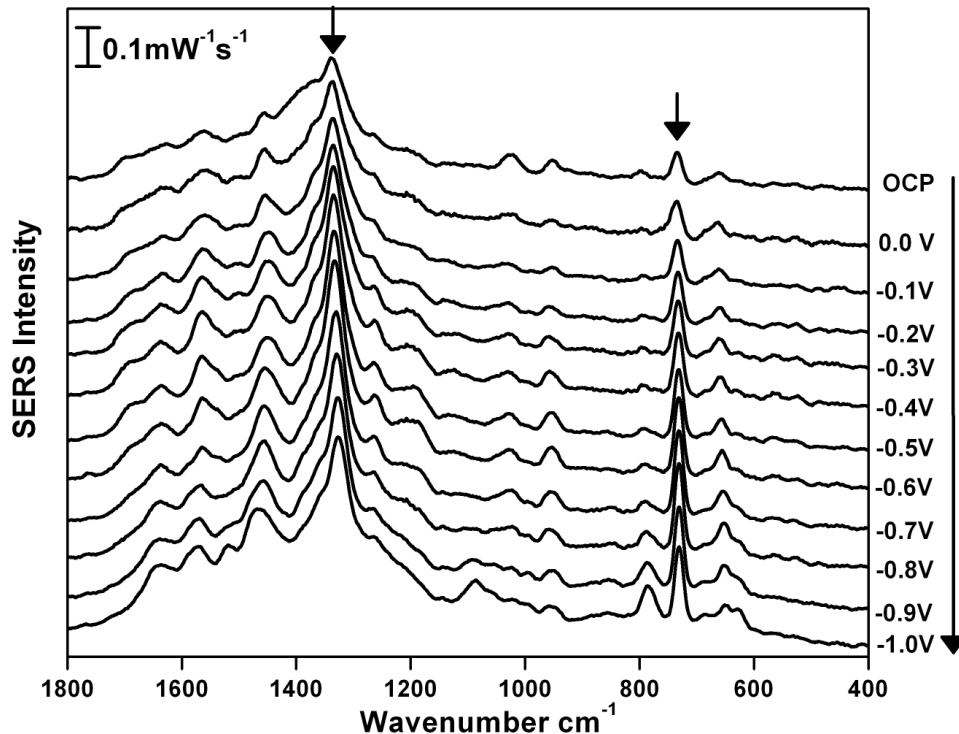
Figure 21: E-SERS cathodic signal for a hybridization study between P_1 and T_1 with the presence of 12-MDA as a back-filled spacer, measured at medium-high (46.5 mW) power for a time interval of 60 seconds. Adenine peaks are indicated by arrows.

2.6.2 Probe 1 + Scrambled Target 1 + 12-MDA

If this hybridization study with backfilling worked as expected, there ought not to be any adenine signal present when performing the same study with the $s.T_1$, since the $s.T_1$ should not be able to bind to the surface directly nor hybridize with P_1. In agreement with this hypothesis, Figure 22 shows that no adenine peaks can be observed for this study. The results show that thiol-backfilling is required to obtain the correct result for these hybridization studies. This is indicative that $s.T_1$ was not non-specifically adsorbed on the AgNP surface, and since it is not the complementary strand for P_1, there was no base-pairing occurring between the nucleotides.
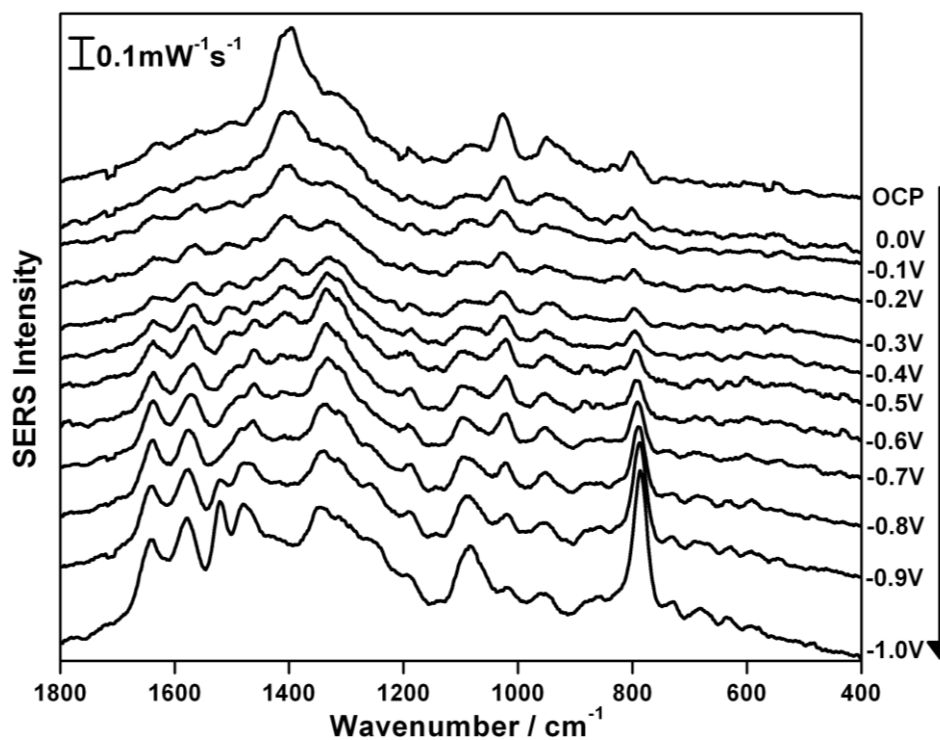
Figure 22: E-SERS cathodic signal for hybridization study between P_1 and s.T_1 with 12-MDA as a back-filled spacer. Measured at medium-high power (46.5 mW) for a time interval of 60 seconds.

2.7 Urine Simulant Studies

2.7.1 Probe 1 + Target 1 + 12-MDA

All the previous studies were conducted in 0.1 M NaF solution, which acts as an ideal electrolyte for performing electrochemical studies because it is relatively inert, and the fluoride ion has a weak specific adsorption on the noble metal surfaces. However, NaF is not biologically relevant, which is an important consideration since this device will be used as a TB biosensor to test real patient samples. The biomarkers will be present in urine, sputum and blood samples of TB patients. Specifically, the DNA fragments from the TB organism, which are the target biomarker for this study, will be secreted into the urine. A commercially available urine simulant, which contains water,

calcium chloride, sodium chloride, magnesium sulfate and urea, was used as an electrolyte instead of NaF to simulate a more realistic clinical sample. The study was conducted under the same parameters and conditions as the study done in NaF. By looking at Figure 23, it is evident that the signal was very noisy; however, the adenine peaks were still present. As the voltage decreased, the signal became less noisy and more peaks appeared. The signal-to-noise ratio was lower than the study conducted in NaF, which might be due to the chloride ions present in the urine simulant. The chloride ions are able to displace the citrate, and possibly the aptamer, because chloride forms a strong covalent bond with silver.
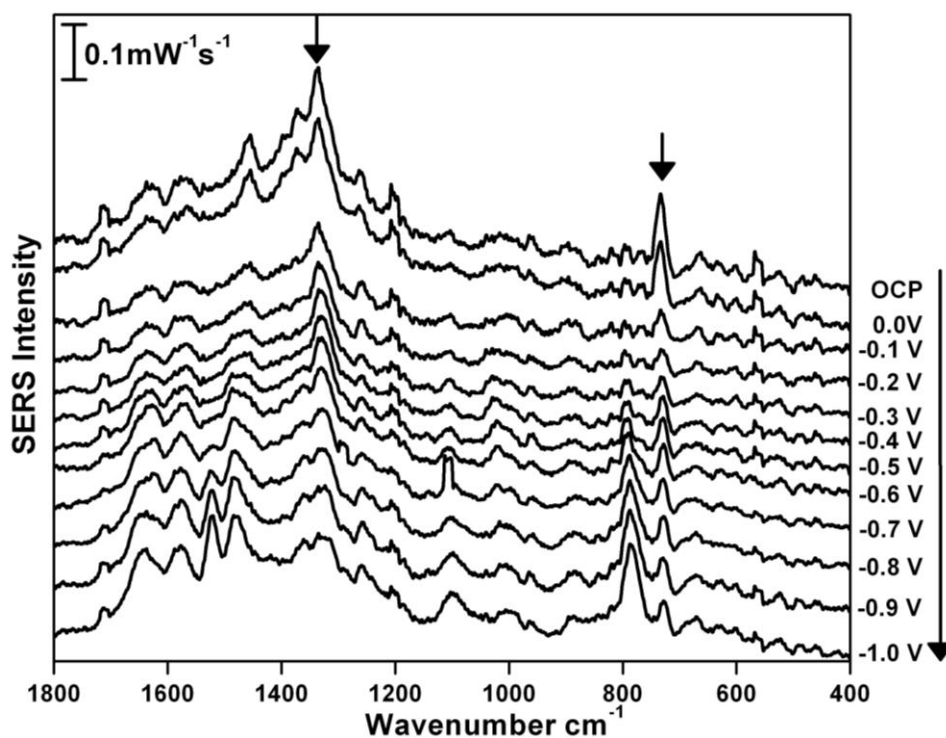
Figure 23: E-SERS cathodic signal of P_1+T_1 +12-MDA conducted in urine simulant at medium-high power (46.5 mW) for a time interval of 60 seconds. Adenine peaks are indicated by arrows.
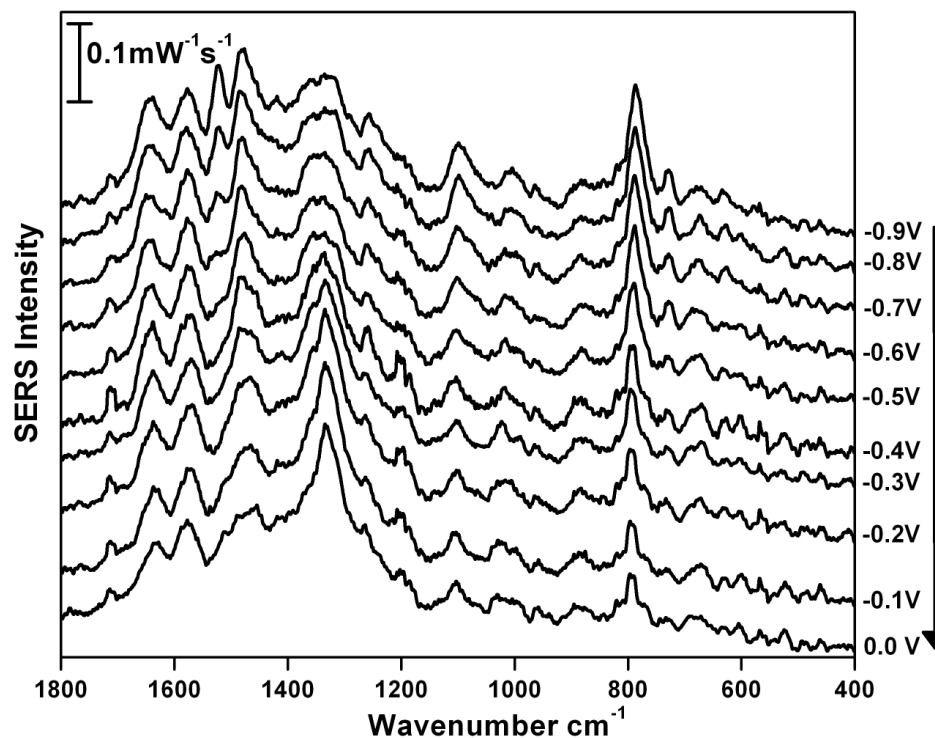
Figure 24: E-SERS anodic signal of P_1+T_1 +12-MDA conducted in urine simulant at medium-high power (46.5 mW) for a time interval of 60 seconds.

A comparison was done between the two electrolyte studies conducted at OCP, as shown in Figure 25. It is obvious that the NaF analyte gave a stronger signal for the hybridization study and the adenine peak was stronger in intensity. Some molecules such as water and urea present in the urine simulant are known to disturb the structure of a double-stranded DNA (ds-DNA) and cause denaturation which might decrease the signal of adenine.[13] Also, some peaks did not appear when urine simulant was used, such as a peak around 662 cm^{-1}, which is indicative of C-S stretch[76] was strongly apparent in NaF but not in the urine simulant, for example.
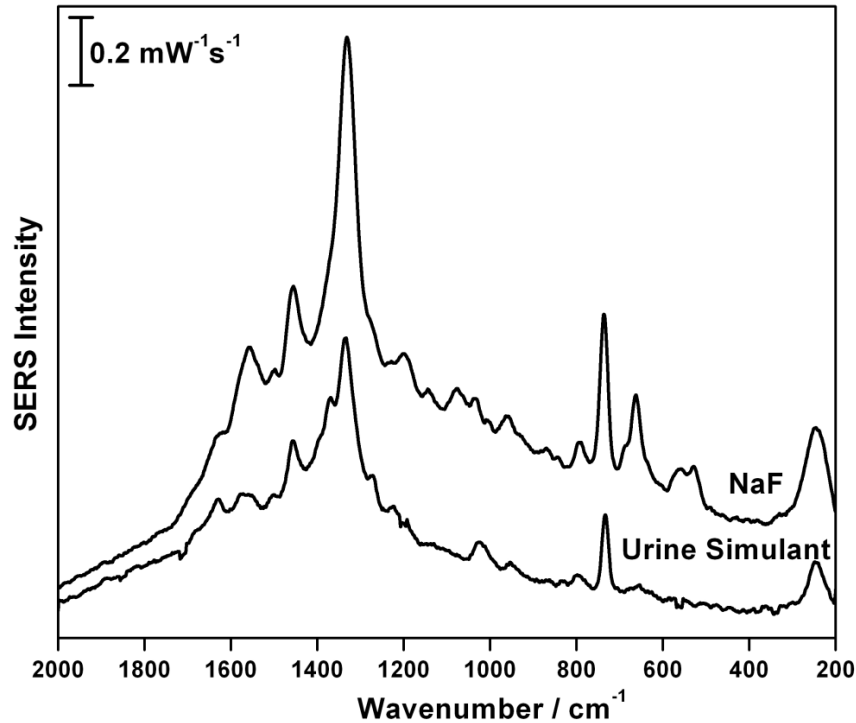
Figure 25: Comparison of SERS spectra at OCP for P_1+T_1 in 0.1M NaF and urine simulant. Both studies were measured at medium-high power (46.5 mW) for a time interval of 60 seconds.

2.8 Dilution Studies

2.8.1 10x Dilution Studies

2.8.1.1 10x of Target 1 (no probe present)

As mentioned previously, the Raman signal can be increased by several orders of magnitude due to the effect of the nanoscale metal surface. However, this enhancement is not uniform over the entire SERS substrate. For example, while a "hot spot" may have a 10^9 enhancement effect, the average enhancement effect over the entire surface may be only 10^4. This lower enhancement is due to the variation of the nanoparticle size within a single nanoparticle batch, and also the non-uniform deposition of the AgNPs on the surface. The original concentration of the target was chosen to be detectable at a low

level of enhancement, and it does not represent the concentration that would be present in a patient's urine sample. Ideally, it would be beneficial if these targets are detectable at the nanomolar concentration scale, which would make the aptasensor competitive with protein-based sensors. The dilution study was done by diluting the original solution used in earlier experiments with phosphate buffer to obtain a 0.416 mM concentration. By looking at Figure 26, it is apparent that at OCP some weak signal was observed, and as the potential decreased, more peaks appeared at -0.5 V. The signal increased, and upon reaching -1.0 V, most of the peaks of the target were present. The anodic signal was also strong, very stable, and the signal was similar to the results obtained at higher concentration.

Figure 26: E-SERS cathodic signal of (10x) diluted T_1 immobilized on a AgNP electrode, measured at medium-high power (46.5 mW) for a time interval of 60 seconds.

2.8.1.2 10x of Target 1 + Probe 1

The probe that is being used in these studies is engineered to have a very high specificity to its complementary strand. This study was performed to test the sensitivity of this probe in order to detect its complementary strand at low concentration, and not hybridization. The 10x diluted T_1 was added to P_1 that had the same concentration as used previously. Figure 27 shows that the adenine peaks around ~730 and 1330 cm^{-1} are apparent at OCP. However, the intensity of the peak is not as strong as the study of $P_1 + T_1$ with higher concentration presented in Figure 16. It indicates that E-SERS is capable of detecting target, even with a 10 fold dilution; although the signal is weaker. This study does not indicate that the P_1 and T_1 are hybridizing, since as shown previously in the absence of a spacer molecule (such as 12-MDA), non-specific binding may be occurring. This study needs to be done in the presence of 12-MDA, and is future work for this project.

Figure 27: E-SERS cathodic signal of P_1+T_1 (10x) immobilized on a AgNP electrode, measured at medium-high power (46.5 mW) for a time interval of 60 seconds.

2.8.2 100x Dilution Studies

2.8.2.1 100x of Target 1 (no probe)

Since the 10 fold dilution studies were successful, and a good signal was obtained at this low concentration, it was imperative to determine the lowest limit of detection for this target. The same solution used earlier was diluted by 100 fold using phosphate buffer to obtain a concentration of 0.0416 mM. By looking at Figure 28, the OCP signal that was collected was very weak, noisy, and it had a lot of background. As the potential was decreased, the signal remained almost the same. Some peaks were present but they were very weak. The anodic signal that was collected showed no improvement in signal intensity, and looked very similar to the cathodic signal. This study was repeated in

duplicate and similar results were achieved. These results indicate that using the current design it will be difficult to detect signal below 0.4 mM, in the absence of a probe molecule.

Figure 28: E-SERS of cathodic signal of (100x) diluted T_1 immobilized on a AgNP electrode, measured at medium-high power (46.5 mW) for a time interval of 60 seconds.

2.8.2.2 100x of Target 1 +Probe 1

Although the signal collected for the 100x dilution for target 1 alone was very weak and had a lot of background, it was still introduced to P_1. In this case, the hope was that the probe would selectively bind to the small amount of target on the surface. As shown in Figure 29, the signal mostly originated from P_1 alone. There were no peaks present for adenine at 730 and 1330 cm^{-1} that would indicate the presence of T_1 on the surface of the electrode. This result was repeated in duplicate, and similar results were

obtained, indicating that a 100x diluted target cannot be detected using the SERS substrate that is currently being used. As mentioned previously, this study needs to be repeated in the presence of 12-MDA as a backfilling spacer.
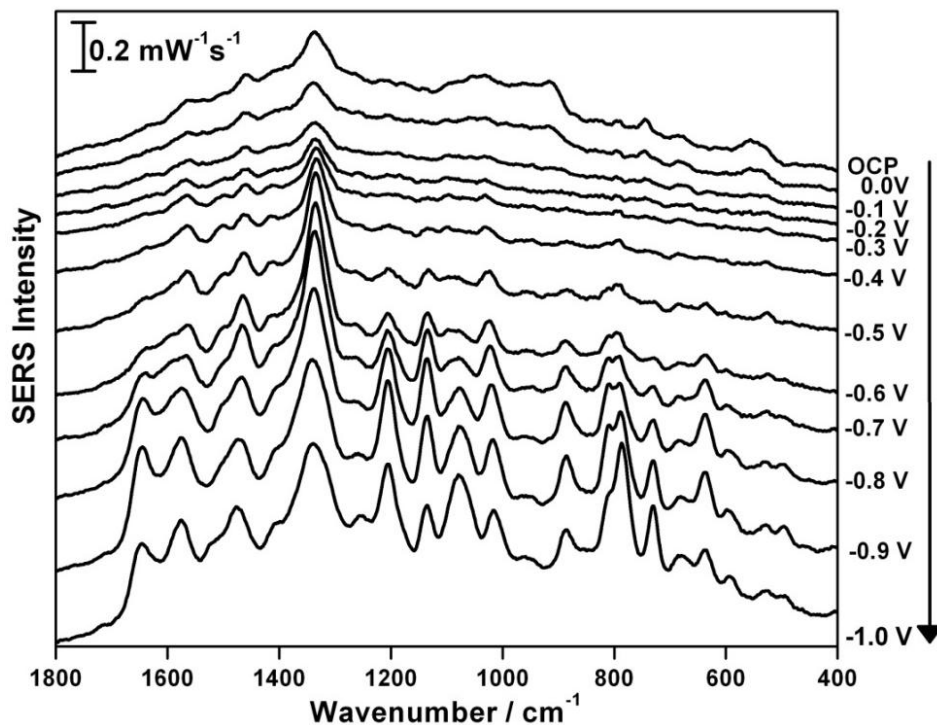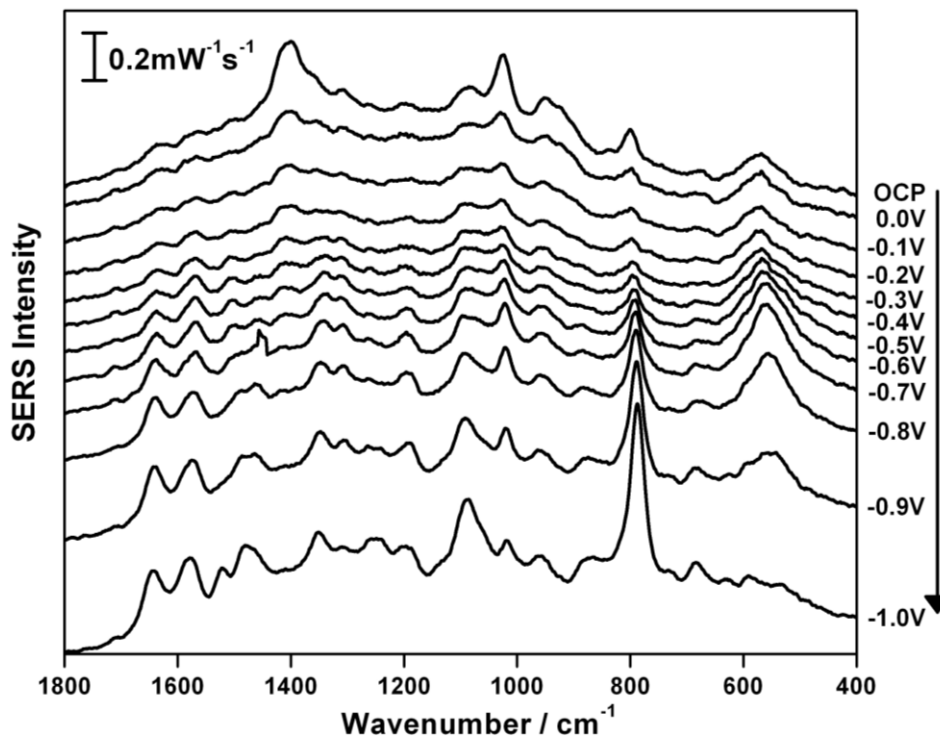

Figure 29: E-SERS cathodic signal of $P_1 + T_1$ (100x) immobilized on a AgNP electrode, measured at medium-high power (46.5 mW) for a time interval of 60 seconds.

2.9 TB Oligonucleotide DNA Studies

2.9.1 TB Oligo without Denaturation

2.9.1.1 Without KCl Treatment

A small fragment of the IS6110 sequence was chosen to be tested first instead of the whole sequence. This TB oligo contains 147 DNA bases, which will be used to bind to P_1, since it contains its complementary strand, which is T_1. This oligo is shipped as double-stranded DNA, and therefore studies were first done using this ds-DNA.

51

However, to bind to the probe properly, this ds-DNA will need to be denatured. In the literature, it was mentioned that ds-DNA has a weakened ability to bind to a SERS substrates, because the DNA bases have already formed base-pairs among themselves, which makes them less accessible to bind to the metal nanoparticles.[73] After thawing for a few minutes, the ds-DNA was directly deposited onto the metal nanoparticles present on the working electrode. By looking at the obtained E-SERS cathodic results in Figure 30, it is evident that at OCP only citrate peaks are present. As the potential was stepped in the cathodic direction, the citrate signal was decreased and was still present until -0.6 V, at which point the entire signal was gone. This observation indicates that the ds-DNA was not able to bind to the SERS substrate through the heterocyclic nitrogenous bases, which verifies the literature observation. Another possibility that could reduce the binding of the ds-DNA is the large number of negatively charged phosphate groups, which can be repelled from the negatively charged surface.
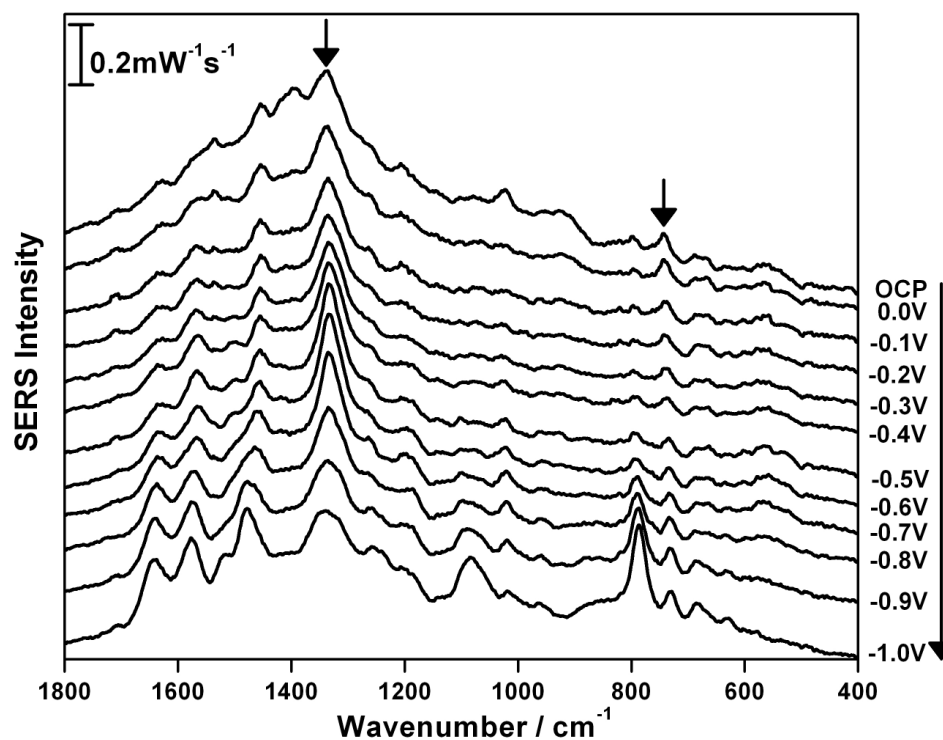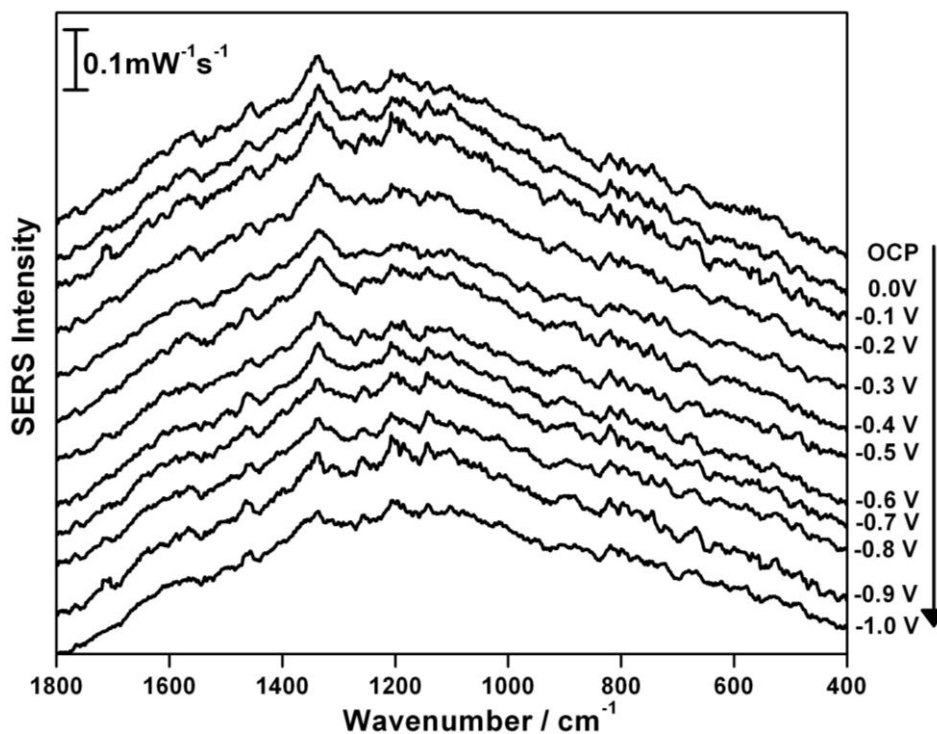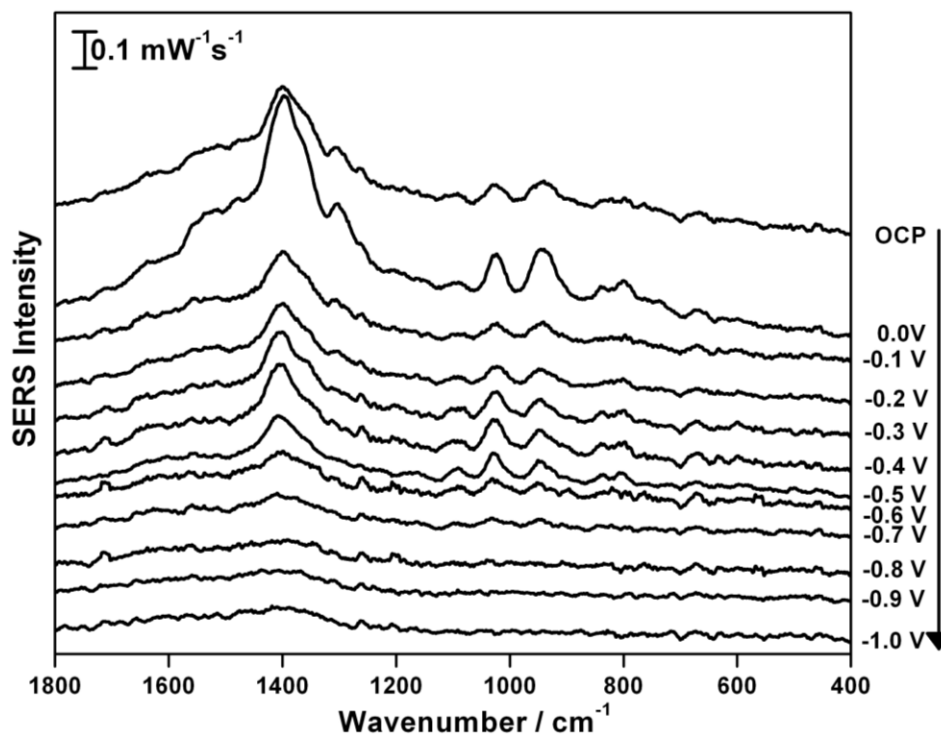
Figure 30: E-SERS cathodic signal of TB oligo immobilized on a AgNP electrode, measured at medium-high power (46.5 mW) for a time interval of 60 seconds.

2.9.1.2 With KCl Treatment

The citrate molecules present on the silver nanoparticles can be removed by several methods. One way to remove the citrate is to apply a negative potential up to -0.8 V to the bare electrode prior to use. Another way is to use a KCl solution whereby the electrode can be incubated in KCl solution, so that the chloride ions displace the citrate. In this case, the electrode was treated with 0.5 M KCl, and then the ds-DNA was introduced. By looking at Figure 31, it is evident that at OCP and up to -0.2 V, there were no peaks present, except for the silver chloride ν(Ag-Cl) peak which is around 246 cm^{-1} [75] that is indicative of the fact that citrate molecules are not present on the AgNP surface. As the potential was decreased, more peaks appeared between 800-1200 cm^{-1}, but they were relatively weak. Figure 32 represents the anodic signal where the potential

53

is stepped in the positive direction, which showed that the peaks are still present, but a lot of background was also present. This observation indicates that KCl pre-treatment of the AgNP SERS substrates can facilitate immobilization of ds-DNA on the surface, due to a reduction in electrostatic repulsion. The next step in this research project is to denature the ds-DNA into ss-DNA by varying experimental conditions such as temperature, pH, and ionic strength.[13]
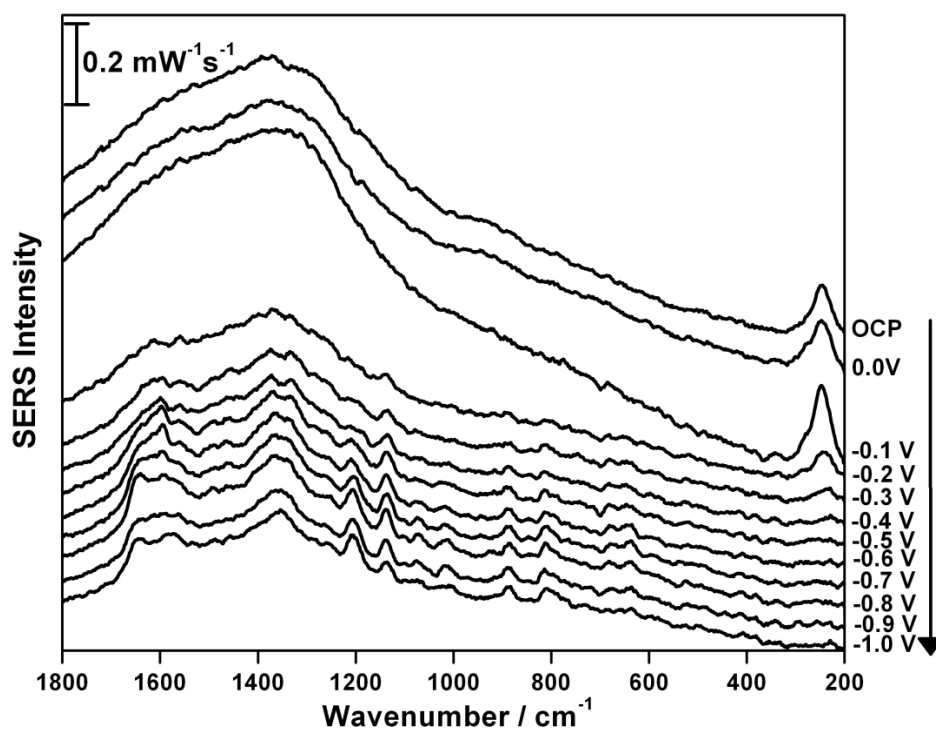
Figure 31: E-SERS cathodic signal of TB oligo with citrate removal using 0.5M KCl for 30 minutes, measured at medium-high power (46.5 mW) for a time interval of 60 seconds.
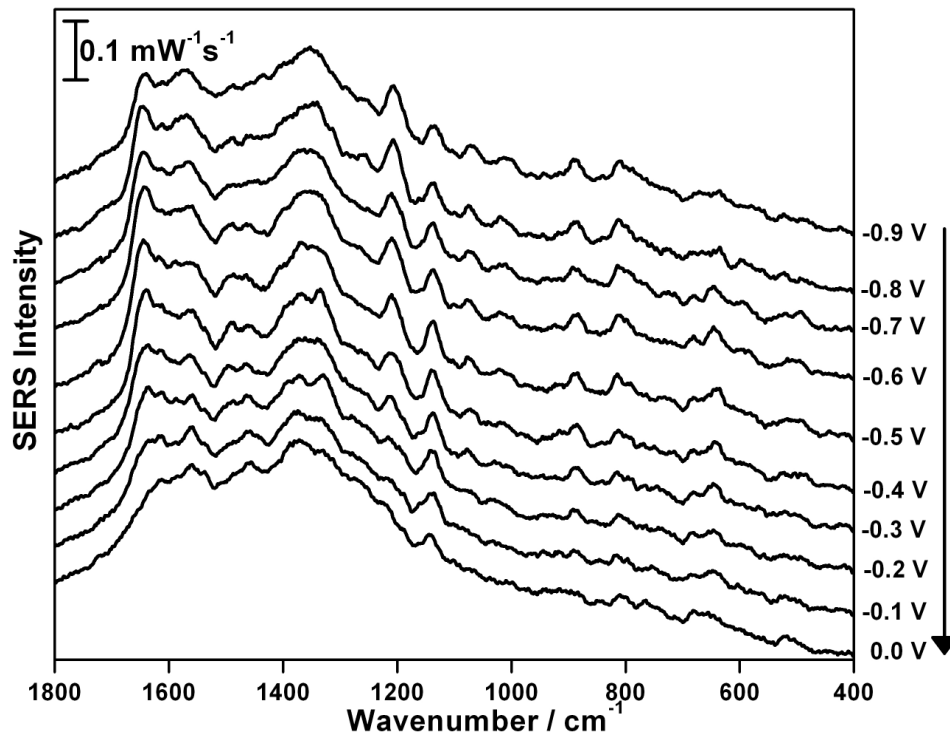
Figure 32: E-SERS anodic signal of TB oligo with citrate removal using 0.5M KCl for 30 minutes, measured at medium-high power (46.5 mW) for a time interval of 60 seconds.

Chapter 3: Conclusion

Raman spectroscopy shows excellent promise over other spectroscopic techniques for the detection of biological analytes which has been demonstrated by the results obtained for both the DNA bases and nucleotides. A unique profile spectrum was observed for each of the four bases, and they were easily distinguished from one other. Each DNA spectrum was characterized by an intense peak around 600-800 cm^{-1} due to the ring breathing vibrations. DNA nucleotides were also detected, but with less intensity due to the phosphate and sugar groups present. However, this problem was overcome by using E-SERS. It was observed that applying a voltage can indeed increase the signal intensity due to reasons such as desorption of citrate, reduction of the S-S bond, increased surface adsorption, and change in conformation of the molecules. Each nucleotide was easily characterized in a mixture solution, which indicates that adenine does not dominate the signal when all nucleotides are present. E-SERS was used to detect three different DNA sequences (P_1, T_1, $s.T_1$), which showed that even non-thiolated aptamers were strongly adsorbed on the SERS substrate. Hybridization studies were successfully conducted between the DNA aptamers P_1 and its complementary strand T_1 with the aid of 12-MDA to act as a spacer SAM for the aptamer. The spacer SAM prevented non-specific binding and surface-induced denaturation of the aptamer. 12-MDA was chosen over other alkanethiols because it showed significant signal stability over a long period of time. These experiments were also conducted in urine simulant, which could be used as an electrolyte for detecting these DNA aptamers; however, the signal was noisier, most likely due to the chloride present.

These results showed promise as a first step in developing an aptasensor for the detection of infectious disease. However, dilution studies were performed to observe the limit of detection, which was approximately 0.4 mM, suggesting that the aptasensor design needs to be improved in order to lower this value. The next step involved the use of the ds-DNA fragment of the IS6110 TB biomarker. The characterization of the ds-DNA using E-SERS was unsuccessful due to i) the presence of large amount of negatively charged phosphate groups, and/or ii) the nucleotides were less accessible for interactions with the SERS substrate. DNA denaturation studies of the TB oligo are currently underway, which will be used to perform hybridization studies with probe 1.

Chapter 4: Future Directions

For future work, the dilution study of P_1 and T_1 should be repeated in the presence of 12-MDA to ensure whether the hybridization can occur at lower concentration. Additionally, the properties of SERS substrates play a role in affecting the signal of the DNA aptamers. Improvement of the limit of detection for the target DNA can be achieved by using different methods to prepare the metal nanoparticles, such as changing the method of deposition on the surface of the electrode, and perhaps the use of a different metal, such as gold. Denaturation studies of the ds-DNA TB oligo will be performed using the widely known protocol of DNA denaturation, which is exposure to high temperature. If the ds-DNA is able to denature and form ss-DNA, the hybridization study with P_1 should be conducted. Furthermore, the size of the DNA fragment might be too long to be detectable by SERS, which can be examined by performing some studies with different target lengths. One of the studies that will be done to test the sensitivity of these DNA aptamers is to perform a hybridization study between the probe and its complementary strand; however the complimentary strand will have a few base mismatches.

Chapter 5: Experimental

5.1 General

All glassware was immersed in an acid bath of 95-98% ACS grade sulfuric acid for several hours and rinsed thoroughly with ultra-pure water (>18.2 MΩ cm^{-1}) from a Milli-Q plus system (Millipore). The same Millipore water was used to prepare all solutions. DNA bases (adenine $\geq$99%, thymine $\geq$99%, cytosine $\geq$99%, and guanine 98%), DNA nucleotides (dAMP 98-100%, dTMP $\geq$99%, dCMP $\geq$98%, dGMP $\geq$99%), sodium citrate, sodium fluoride, and 12-MDA were all purchased from Sigma-Aldrich (St. Louis, MO, USA). Silver nitrate (99.9995%) was purchased from Alfa Aesar (Wardhill, MA, USA). DNA sequences (probe 1, target 1, and scrambled target 1) were purchased from Integrated DNA Technology (IDT). The TB DNA aptamer sequence was developed via the SELEX process in the laboratory of our colleague, Dr. Jonathan Blackburn, at the University of Cape Town, South Africa.

5.2 Nanoparticle Synthesis and Characterization

Citrate reduced silver colloids were prepared using the standard Lee and Meisel method [66] and were found to have a peak absorption wavelength of ~420 nm and a full width at half maximum (fwhm) of ~100 nm. This nanoparticle synthesis must have minimal exposure to light, because the reaction is photosensitive. The preparation of citrate-reduced silver colloids was done using silver nitrate (99.9995%) and trisodium citrate. First, 0.09 g of silver nitrate was added to 500 mL of Millipore water and brought to a vigorous boil in a covered beaker with stirring. Next, 10 mL of a 1 % w/w trisodium citrate was then added to reduce the silver, and left to boil for 30 minutes. After a set

amount of time, the reaction mixture was removed from heat and allowed to cool. After

cooling, 1 mL aliquots of the colloidal nanoparticles were placed in tubes to be

centrifuged 10 times for 15 minutes at 3600 rpm to concentrate and aggregate the

colloids. Each time, the supernatant was carefully removed without removing any of the

nanoparticles, and a fresh aliquot of colloidal suspension was added. Once centrifugation

was complete, the AgNPs were applied to the screen printed electrodes (SPEs), as

discussed below.

5.3 Construction of AgNP Electrodes

Carbon SPEs (15 x 61 x 0.36 mm) were purchased from Pine Research

Instrumentation (Durham, NC, USA) which consist of a silver/silver chloride (Ag/AgCl)

RE, a carbon CE, and carbon WE. These SPEs were functionalized by depositing three 5

µL layers of the concentrated silver nanoparticle (AgNP) suspension onto the carbon WE

(5 x 4 mm) using a micropipette. The electrodes were left to dry completely between

deposition of the AgNP layers, and the final layer was allowed to dry completely before

the electrode was used.

5.4 Preparation of Nucleic Acids

5.4.1 DNA Aptamers (Probe 1, Target 1, scrambled Target 1)

The DNA aptamers were engineered using the SELEX process at the University

of Cape Town, South Africa. The DNA aptamers were then synthesized and shipped

from IDT in the form of pellets stored in small vials. The centrifuge tubes were mixed

well using a vortex to make sure the entire DNA sample was on the bottom of each vial.

All the DNA aptamer solutions were prepared in fresh phosphate buffer with a pH of 7.4. A certain amount of phosphate buffer was added to each vial to make up a chosen concentration of each DNA aptamer. The exact amount of phosphate buffer added, as well as the concentration of each solution is indicated as: P_1 (230 µl, 2.08 mM), T_1 (230 µl, 4.16 mM), s.T_1 (230 µl, 2.28 mM). Each vial was mixed well to make sure the DNA aptamer was completely dissolved in the phosphate buffer, and then the tubes were stored at 4 ℃ prior to use.

5.4.2 TB Oligonucleotide

The TB oligo fragment was shipped in a small vial in the form of pellet; the vial was centrifuged (~ 1 minute) at 3600 rpm to make sure the pellet was at the bottom of the vial. To prepare the oligo, 37 µL of Millipore water was added to the vial that contained 370 nanograms of the oligo, to make up a concentration of 10 ng/µL. The tube was left upright for one hour at room temperature to resuspend the DNA oligo. The tube was centrifuged again for 5 minutes at 3600 rpm. Dilution series were also performed to obtain a concentration of 1 ng/µL of the DNA oligo, this was done by taking 10 µL of stock solution into a new vial and diluting it with 100 µL of Millipore water. Lastly, 10 µL aliquots were taken out and placed in 10 different tubes, and stored at -20 ℃ with the rest of the stock solution.

5.5 Raman Spectroscopy

5.5.1 Instrumentation

All experiments except the SAM studies using 12-MDA were conducted using a system that consists of a DeltaNu benchtop dispersive Raman spectrometer equipped with an air-cooled CCD, a 785 nm diode laser, an optics extension tube, and a right angle optics attachment (Intevac Photonics, Santa Clara, USA). The optics extension was used to detect the analyte in solution or on the surface of the SPEs, while the right angle attachment was used to detect solid analyte when placed on a microscope slide. The focal point between the attachments and the sample was approximately 1.6 cm. The samples were collected at laser powers between 22.3-55.9 mW and for acquisition times between 30-60 seconds. The spectrometer resolution was 5 cm^{-1} and the spectral range was between 200-2000 cm^{-1}. This benchtop Raman spectrometer was used for all spectroscopic measurements, unless otherwise indicated. For spectral processing and data analysis, the software program Origin 8.1 was used on a standard PC. All the data measured were corrected for the time and power, and also smoothed using adjacent-averaging smoothing methods of 15 points. Origin 8.1 is produced by OriginLab Corporation, Northampton, MA, USA.

A handful of the studies presented in this work (i.e. SAM studies) were conducted using a DXR Smart Raman Spectrometer (Thermo Fisher Scientific, Mississauga, ON, Canada). This spectrometer is equipped with two different laser excitation wavelengths (532 nm and 780 nm). The maximum power used at 532 nm is 10 mW, while the maximum power used at 780 nm is 150 mW. This spectrometer can be fitted with two

different gratings, a full range grating with a resolution of 5 cm^{-1}, and a high resolution grating with a resolution of 3 cm^{-1}. It has a 10 μm in diameter laser spot size, and is equipped with an air-cooled CCD detector.

5.6 Electrochemical Set-up

The Pine Research Instrumentation portable USB Wavenow potentiostat/galvanostat (Durham, NC, USA) was used for conducting electrochemical measurements. This potentiostat/galvanostat is connected to the computer, which uses software for signal processing and the setup of electrochemical parameters. The electrochemical software is Aftermath Data Organizer (version 1.2.4361) produced by Pine Research Instrumentation.

5.6.1 Cyclic Voltammetry (CV)

Cyclic Voltammetry (CV) was conducted at the end of each experiment to assess film quality and probe redox behavior. The CV parameters used were the same for all experiments; the initial and upper potentials were set to 0.0 V, the sweep rate was set to 50 mV/s, and a lower potential of -1.0 V was used, and the number of segments was set to 10.

5.6.2 E-SERS

For E-SERS, the applied potential ranged from 0.0 V to -1.0 V in increments of 0.1 V for a time interval of 60 seconds. Positive voltages were avoided in order to prevent oxidation of the silver surface. The voltage was stepped first in the cathodic direction (0.0 V to -1.0 V), and then returning in the anodic direction (-1.0 V to 0.0 V).

The voltammetry cell, also from Pine Research Instrumentation, was used as the spectroelectrochemical cell. The cell design consists of a standard disposable glass vial and a special mini USB adapter that is made to fit the SPEs. A diagram of the electrochemical set-up is shown in Figure 33. All potentials are reported versus the Ag/AgCl reference electrode, unless otherwise indicated.
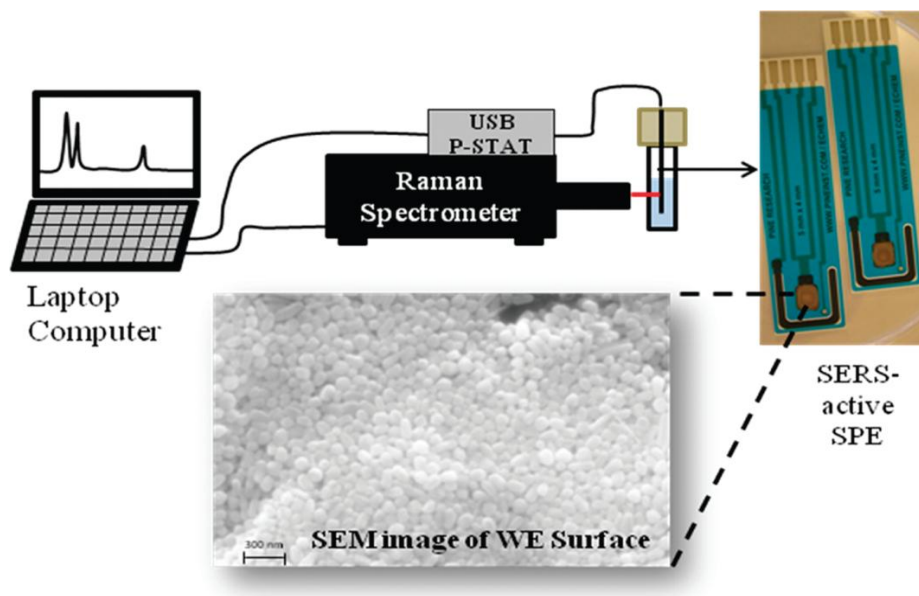
Figure 33: Schematic representation of the portable electrochemical surface-enhanced Raman setup. The inset shows an SEM image of the AgNP electrode surface.[55]

For most of the conducted experiments, the analyte of interest was immobilized on the AgNP electrode; however, for the DNA base/nucleotides studies, a bare AgNP electrode was immersed in 0.1 M NaF electrolyte solution, which contained the analyte. For spectroelectrochemistry (E-SERS), these electrodes were placed in the special adapter for the cell vial that connects it to the USB Wavenow potentiostat. The electrodes were then analysed using the Raman spectrometer to ensure that they were at the focal point of the laser before the electrolyte was added. Once focused, the Raman

spectral analysis and the potentials were applied in concert, acquiring the spectrum for one minute at each potential.

5.7 Preparation of aptamer monolayers for E-SERS

5.7.1 Deposition of Aptamer SAM

The AgNP electrodes were usually prepared several days in advance of conducting experiments. The DNA aptamer solution was taken out of the fridge and mixed well using a vortex mixer for about a minute. Using a micropipette, 10 µL of the solution was taken out and deposited on the surface of the AgNP. The electrode was left to dry in air for 12 hours. The surface was then rinsed gently with Millipore water to remove any excess unbound DNA aptamer. The electrode was again left to air dry for 10 minutes before performing E-SERS studies.

5.7.2 Hybridization Studies (Probe1+Target 1) (Probe 1+scrambled Target 1)

For the hybridization studies, 10 µL of P_1 was added to the surface of the AgNP electrode following the same procedure mentioned above. After leaving it to dry overnight, 10 µL of T_1 was then added to the AgNP electrode and left to dry in air overnight as well. The electrode was then rinsed gently with Millipore water, and left to dry in air before performing E-SERS.

5.7.3 Hybridization Studies + Thiol-backfilling with Spacer

These hybridization studies are the same as those mentioned in the hybridization study section; however, a thiol was introduced as a back-filled spacer. After depositing P_1 on the surface, the electrode was then immersed in a 1.0 mM ethanolic solution of

12-MDA for 2 hours. The electrode was then rinsed with ethanol to remove any excess 12-MDA that was not adsorbed on the surface. T_1 was added onto the AgNP electrode after it had dried, and the same procedure was followed as mentioned above.

5.8 E-SERS Preparation on TB Oligonucleotide

5.8.1 Oligonucleotide Study without Denaturation

A tube containing the TB oligo solution was taken out of the freezer and left to thaw for a couple of minutes before performing any studies. Using a micropipette, the 10 µL present in the vial was deposited on a AgNP electrode and left to dry. The next day, the electrode was rinsed gently with Millipore water, and left to dry in air before performing the experiment. However, KCl was also used in some studies to displace the citrate present on the surface of the silver nanoparticles. This was done by incubating the AgNP electrode in 0.5 M KCl for 30 minutes, then the surface of the AgNP electrode was rinsed with Millipore water and left to dry. The TB oligo was then deposited on the surface of the electrode and same procedure was followed as mentioned previously in section 5.7.1.

Chapter 6: References

1) Duijvesz, D.; Luider, T.; Bangma, C. H.; Jenster, G. *Eur. Urol.* **2011**, *59*, 823-831.

2) Gloyn, A. L.; Faber, J. H.; Malmodin, D.; Thanabalasingham, G.; Lam, F.; Ueland, P. M.; McCarthy, M. I.; Owen, K. R.; Baunsgaard, D. *PLoS ONE* **2012***, 7*, 1-7.

3) Gubala, V.; Harris, L. F.; Ricco, A.J.; Tan, M. X.; Williams, D.E. *Anal. Chem.* **2012**, *84*, 487-515.

4) World Health Organization, Health Topic: Tuberculosis. http://www.who.int/topics/tuberculosis/en/ (accessed on March 23, 2013).

5) Finer, R. K. *Deadly Diseases and Epidermics: Tubercolusis*. Infobase Publishing: New York, 2003; pp 16,24,26

6) Coros, A.; DeConno, E.; Derbyshire, K. M. *J. Bacteriol.* **2008**, *190*, 3408-3410.

7) Cleveland Clinic: Tuberculosis. http://www.clevelandclinic.org/health/health-info/docs/1100/1160.asp (accessed on March 23, 2013).

8) Centers for Disease Control and Prevention, Tuberculosis. http://www.cdc.gov/tb/topic/basics/default.htm (accessed on March 23, 2013).

9) Grand Challenges Canada, Point-of-Care Diagnostics Meeting, Seattle, Washington, **May 8-11, 2012**.

10) World Health Organization, Health Topic: Tuberculosis. http://www.who.int/features/factfiles/tuberculosis/en/index.html (accessed on March 23, 2013).

11) Medical News Today, Tuberculosis. http://www.medicalnewstoday.com/articles/8856.php (accessed on March 23, 2013).

12) Phillips M.; Basa-Dalay V.; Bothamley G.; Cataneo R. N.; Lam P. K.; Natividad M. P. R.; Schmitt P.; Wai J. *Tuberculosis* **2010**, *90*, 145-151.

13) Garrett, R. H.; Grisham, C. M. *Biochemistry*; Brooks/Cole: Belmont, 2013; pp 313-319, 354.

14) Sun, X.; He, P.; Liu, S.; Ye, J.; Fang, Y. *Talanta* **1998**, *47*, 487-495.

15) Guo, Z.; Yang, F.; Zhang, L.; Zheng, X. *Sens.Actutator, B.* **2013**, *177*, 316-321.

16) Tersch, C.; Lisdat, F. *Electrochim. Acta* **2011**, *56*, 7673-7679.

17) Tuerk, C.; Gold, L. *Science* **1990**, *249*, 505-510.

18) Ellington, A.D.; Szostak, J.W. *Nature* **1990**, *346*, 818-822.

19) Robertson, D. L.; Joyce, G. F. *Nature* **1990**, *344*, 467-468.

20) Velasco-Garcia, M. N.; Missailidis, S. *Gene Ther. Mol. Biol.* **2009**, *13*, 1-9.

21) Iliuk, A. B.; Hu, L.; Tao, W. A. *Anal. Chem.* **2011**, *83*, 4440-4452.

22) Katilius, E.; Flores, C.; Woodbury, N. W. *Nucleic Acids Res.* **2007**, *35*, 1-10.

23) Tombelli, S.; Minunni, M.; Mascini, M. *Biosens. Bioelectron.* **2005**, *20*, 2424-2434.

24) Neumann, O.; Zhang, D.; Tam, F.; Lal, S.; Wittung-Stafshede, P.; Halas, N. J. *Anal. Chem.* **2009**, *81*, 10002-10006.

25) Lee, J. F.; Stovall, G. M.; Ellington, A. D. *Curr. Opin. Chem. Biol.* **2006**, *10*, 282-289.

26) Medley, C. D.; Bamrungsap, S.; Tan, W.; Smith, J. E. *Anal. Chem.* **2011**, *83*, 727-734.

27) Negri, P.; Chen, G.; Kage, A.; Nitsche, A.; Naumann, D.; Xu, B.; Dluhy, R. A. *Anal. Chem.* **2012**, *84*, 5501-5508.

28) Levy-Nissenbaum, E.; Radovic-Moreno, A. F.; Wang, A. Z.; Langer, R.; Farokhzad, O. C. *Trends Biotechnol.* **2008**, *26*, 442-449.

29) Graham, D.; Stevenson, R.; Thompson, D. G.; Barrett, L.; Dalton, C.; Faulds, K. *Faraday Discuss.* **2011**, *149*, 291-299.

30) Djordjevic, M. *Biomol. Eng.* **2007**, *24*, 179-189.

31) Stoltenburg, R.; Reinemann, C.; Strehlitz, B. *Biomol. Eng.* **2007**, *24*, 381-403.

32) Kimmel, D. W.; LeBlac, G.; Meschievitz, M. E.; Cliffel, D. E. *Anal. Chem.* **2012**, *84*, 685-707.

33) Yoo, E. H.; Lee, S. Y.; *Sensors* **2010**, *10*, 4558-4576.

34) Clark, L. C.; Lyons Jr., C. Ann. N. Y. *Acad. Sci.* **1962**, *102*, 29-45.

35) Crouch, E.; Cowell, D. C.; Hoskins, S.; Pittson, R. W.; Hart, J. P. *Biosens. Bioelectron.* **2005**, *21*, 712-718.

36) Tichoniuk, M.; Ligaj, M.; Filipiak, M. *Sensors* **2008**, *8*, 2118-2135.

37) Li, K.; Lai, Y.; Zhang, W.; Jin, L. *Talanta* **2011**, *84*, 607-613.

38) Lee, S.; Song, K. M.; Jeon, W.; Jo, H.; Shim, Y. B.; Ban, C. *Biosens. Bioelectron.* **2012**, *35*, 291-296.

39) Flechsig, G. U.; Peter, J.; Voss, K.; Gründler, P. *Electrochem. Commun.* **2005**, *7*, 1059-1065.

40) Zhao, Y. D.; Pang, D. W.; Hu, S.; Wang, Z. L.; Cheng, J. K.; Dai, H. P. *Talanta* **1999**, *49*, 751-756.

41) Green, C. ; Huggett, J. F.; Talbot, E.; Mwaba, P.; Reither, K.; Zumla, A. *Lancet. Infect. Dis.* **2009**, *9*, 505-511.

42) McEvoy, C. R. E.; Falmer, A. A.; Gey van Pittius, N. C.; Victor, T. C.; van Helden, P. D.; Warren, R. M. *Tuberculosis* **2007**, *87*, 393-404.

43) Van Soolingen, D.; De Haas, P. E. W.; Hermans, P. W. M.; Groenen, P. M. A.; Van Embden, J. D. A. *J. Clin. Microbiol.* **1993**, *31*, 1987-1995.

44) Maurya, A. K.; Kant, S.; Nag, V. L.; Kushwaha, R.; Dhole, T. N. *Indian J. Med. Microbiol.* **2012**, *30*, 182-186.

45) Savelkoul, P. H. M.; Catsburg, A.; Mulder, S.; Oostendorp, L.; Schirm, J.; Wilke, H.; Van der Zanden, A. G. M.; Noordhoek, G. T. *J. Microbiol. Methods* **2006**, *66*, 177-180.

46) Fomukong, N.; Beggs, M.; El Hajj, H.; Templeton, G.; Kisenach, K.; Cave, M. D. *Tubercle Lung Dis.* **1998**, *78*, 109-116.

47) Siddiqi, N.; Shamim, M.; Amin, A.; Chauhan, D. S.; Das, R.; Srivastava, K.; Singh, D.; Sharma, V.D.; Katoch, V. M.; Sharma, S. K.; Hanief, M.; Hasnain, S. E. *Infect. Genet. Evol.* **2001**, *1*, 109-116.

48) Haas, W. H.; Butler, W. R.; Woodley, C. L.; Crawford, J. T. *J. Clin. Microbiol.* **1993**, *31*, 1293-1298.

49) Borrell, S.; Throne, N.; Espanol, M.; Mortimer, C.; Orcau, À.; Coll, P.; Charbia, S.; Gonzalez-Martin, J.; Arnold, C. *Tuberculosis* **2009**, *89*, 233-237.

50) Wang, J. *Analytical Electrochemistry, 2nd ed.*; Wiley-VCH: New York, 2000; pp 1, 2, 28, 100-103,114.

51) Bard, A. J.; Faulkner, L. R. *Electrochemical methods: Fundamentals and applications, second edition*; John Wiley & Sons, Inc.: New York, 2001; p 26.

52) Derek, P. *First Course in Electrode Processes, 2nd ed.*; Royal Society of Chemistry: Cambridge, 2009, p139.

53) Movasaghi Z.; Rehman S.; Rehman I. U. *Appl. Spectrosc. Rev.* **2007**, *42*, 493-541.

54) Harris, D.C.; Bertolucci, M. D. *Symmetry and Spectroscopy: An Introduction to Vibrational and Electronic Spectroscopy*; Dove Publication: New York, **1989**, pp 93-97, 151-159.

55) Robinson, A. M.; Harroun, S. G.; Bergman, J.; Brosseau C. L. *Anal. Chem.* **2012**, *84*, 1760-1764.

56) Doering, W. E.; Piotti, M. E.; Natan, M. J.; Freeman, R. G. *Adv. Mater.* **2007**, *19*, 3100-3108.

57) Bantz, K. C.; Meyer A.F.; Wittenberg A.J.; Im H.; Kutulus Ö.; Lee S.H.; Lindquist N.C.; Oh S.-H.; Haynes C.L. *Phys. Chem. Chem. Phys.* **2011**, *13,* 11551-11567.

58) Fleischmann, M.; Hendra, P. J.; McQuillan, A. J. *Chem. Phys. Lett.* **1974**, *26*, 163-166.

59) Jeanmaire, D. L.; Van Duyne, R. P. J. *Electroanal. Chem.* **1977**, *84*, 1.

60) Das, G.; Patra, N.; Gopalakrishnan, A.; Zaccaria, R. P.; Toma, A.; Thorat, S.; Fabrizio, E. D.; Diaspro, A.; Salerno, M. *Analyst* **2012**, *137*, 1785-1792.

61) Hering, K.; Cialla, D.; Ackermann, K.; Dörfer, T.; Möller, R.; Schneidewind, H.; Mattheis, R.; Fritzsche, W.; Rösch, P.; Popp, J. *Anal. Bioanal. Chem.* **2008**, *390*, 113-124.

62) Stiles, P. L.; Dieringer, J. A.; Shah, N. C.; Van Duyne, R. P. *Annu. Rev. Anal. Chem.* **2008**, *1*, 601-626.

63) Porter, M. D.; Lipert, R. J.; Siperko, L. M.; Wang, G.; Narayanan, R. *Chem. Soc. Rev.* **2008**, *37*, 1001-1011.

64) Sulka, G. D. Highly Ordered Anodic Porous Alumina Formation by Self-Organized Anodizing. In *Nanostructured Materials in Electrochemistry*; Eftekhari, A., Ed.; Wiley-VCH, Weinheim, Germany, 2008; p 1.

65) Zhang, J. Z. *Optical Properties and Spectroscopy of Nanomaterials*. World Scientific Publishing Co. Pte. Ltd.: Singapore, 2009; p 1.

66) Lee, P. C.; Meisel, D. J. *Phys. Chem*. **1982**, *86*, 3391-3395.

67) Moskovits, M. J. *Chem. Phys*. **1982**, *77*, 4408-4416.

68) Le Ru, E. C.; Meyer, S. A.; Artur, C.; Etchegoin, P. G.; Grand, J. ; Lang, P. ; Maurel, F. *Chem. Commun*. **2011**, *47*, 3903-3905.

69) Feng, S.; Chen, R.; Lin, J.; Pan, J.; Chen, G.; Li, Y.; Cheng, M.; Huang, Z.; Chen, J.; Zeng, H. *Biosens. Bioelectron.* **2010**, *25*, 2414-2419.

70) Goodall, B. L.; Robinson, A. M.; Brosseau, C. L. *Phys.Chem.Chem.Phys.* **2013**, *15*, 1382-1388.

71) Chen, J.; Jiang, J.; Gao, X.; Liu, G.; Shen, G.; Yu, R. *Chem. Eur. J.* **2008**, *14*, 8374-8382.

72) Gelder, J. D.; Gussem, K. D.; Vandenabeele, P.; Moens, L. *J. Raman. Spectrosc.* **2007**, *38*, 1133-1147.

73) Bell, S. E. J.; Sirimuthu, N. M. S. *J. Am. Chem. Soc*. **2006**, *128*, 15580-15581.

74) Venkataramanan, M.; Skanth, G.; Bandyopadhyay, K.; Vijayamohanan, K.; Pradeep, T. *J. Colloid Interface Sci.* **1999**, *212*, 553-561.

75) Munro, C. H.; Smith, W. E.; Garner, M.; Clarkson, J.; White, P. C. *Langmuir* **1995**, *11*, 3712-3720.

76) Bensebaa, F.; Zhou, Y.; Brolo, A. G.; Irish, D. E.; Deslandes, Y.; Kruus, E.; Ellis, T. H. *Spectrochim. Acta, Part A* **1999**, *55*, 1229-1236.

77) Socrates, G. *Infrared and Rama Characteristic Group Frequncies: Tables and Charts, 3rd ed.*; John Wiley & Sons, LTD.: Chichester, England, **2001**, pp 26, 210-212.

78) Protein Data Bank, Structure of the CFP10-ESAT6 complex from Mycobacterium Tuberculosis.
 http://www.rcsb.org/pdb/explore.do?structureId=3FAV (accessed on March 29, 2013).

79) Protein Data Bank, Crystal structure of native catalase-peroxidase KATG at pH 8.0. http://www.rcsb.org/pdb/explore.do?structureId=2b2o (accessed on March 29, 2013).

80) Treumann, A.; Homans, S. The structure of *Mycobacterium tuberculosis* liparabinomannan (LAM).
http://www.astbury.leeds.ac.uk/Report/2000/Homans.micro.3.html (accessed on March 29, 2013).

81) Institute of Molecular Genetics of Montpellier (IGMM).
http://www.igmm.cnrs.fr/spip.php?rubrique89 (accessed on March 29, 2013).

Appendix:
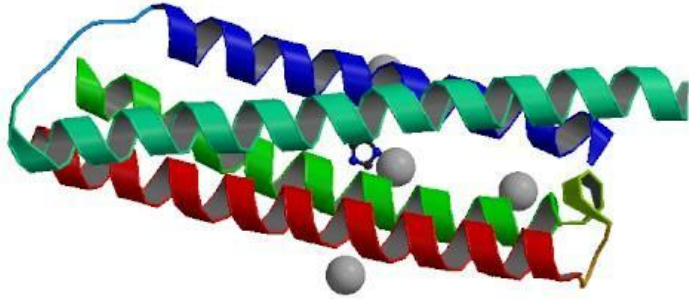
Figure A1: 6 kDa Early Secretory Antigen (ESAT6).[78]
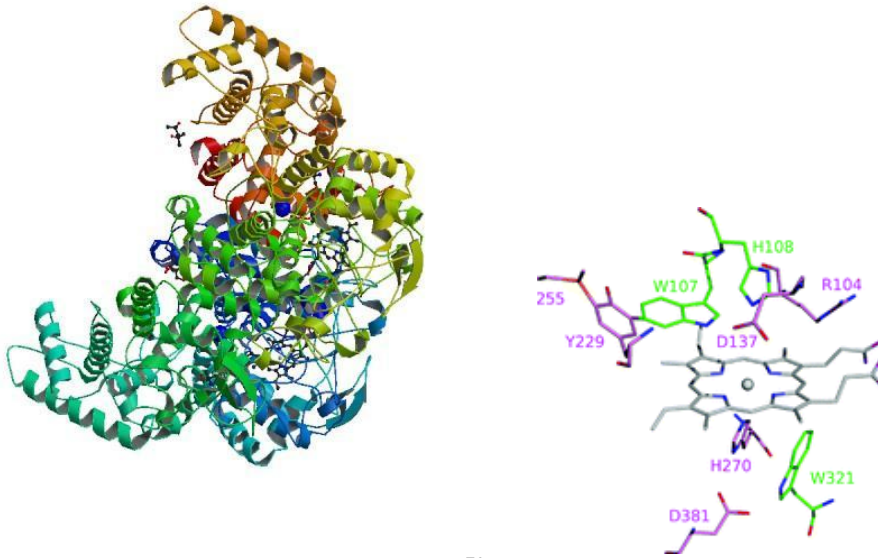
Figure A2: KatG catalase-peroxidase.[79]

α–Mannose
Inositol
α-Arabinose
β-Arabinose
Phosphate
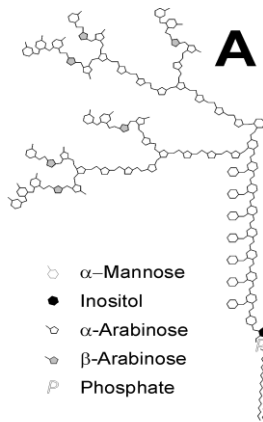

Figure A3: Lipoarabinomannan (LAM). [80]   **Figure A4:** IS6110 DNA Fragments.[81]
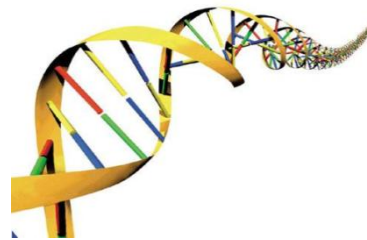
Table A-1: Peaks present in the adenine Raman spectrum and corresponding assignment.

Peak (cm^{-1})	Assignment[53]
331(*m*)	-
536(*m*)	-
623(*m*)	**C-C twist of aromatic ring**
723(*s*)	**Adenine ring breathing mode of DNA**
899(*w*)	-
943(*m*)	-
1024(*w*)	-
1127(*m*)	**v (C-N)**
1251(*ms*)	**-**
1334(*s*)	-
1374(*m*)	**Adenine** (ring breathing mode of the DNA),
1422(*w*)	**Adenine** (ring breathing modes of the DNA),
1485(*m*)	**Adenine** (ring breathing modes in DNA) nucleotide acid purine bases (A)

Table A-2: Peaks present in the guanine Raman spectrum and corresponding assignment.

Peak (cm^{-1})	Assignment[53]
399(*m*)	-
496(*m*)	-
562(*m*)	-
650(*s*)	-
938(*s*)	**C-C** stretch backbone
1049(*w*)	-
1160(*w*)	-
1187(*w*)	-
1235(*ms*)	**Amide III**
1266(*ms*)	**Amide III** (arising from the coupling of C-N stretching and N-H bonding)
1362(*m*)	**Guanine**
1391(*m*)	**C-H** rocking

Peak (cm⁻¹)	Assignment
1422(*m*)	**G** (ring breathing modes of the DNA bases)
1470(w)	**C=N stretching**
1479(w)	**Amide II** (largely due to coupling of C-N and in-plane bending of the N-H group)
1553(m)	**Amide II**
1676(w)	**Amide I**

Table A-3: Peaks present in the cytosine Raman spectrum and corresponding assignment.

Peak (cm^{-1})	Assignment[53]
548(*m*)	-
599(*m*)	-
790(*s*)	-
972(*w*)	v(**C-C**) wagging
990(*w*)	-
1108(*m*)	-
1250(*s*)	**Cytosine** (NH_2)
1278(*s*)	**Amide III**
1363(*mw*)	-
1461(*w*)	-
1535(*w*)	**Amide carbonyl group vibrations and aromatic hydrogens, Amide III**
1655(*w*)	**Amide I**

Table A-4: Peaks present in the thymine Raman spectrum and corresponding assignment.

Peak (cm^{-1})	Assignment[53]
479(*w*)	**DNA**
558(*w*)	-
617(*m*)	-
806(*w*)	-
984(*m*)	-
1216(*w*)	**C-N** stretching
1255(*w*)	**C-N** in plane stretching, **Thymine** (ring breathing modes of the DNA bases), **Amide III**
1371(*s*)	**Thymine** (ring breathing modes of the DNA bases)

1434(*w*)	-
1460(*w*)	**CH$_3$** deformation
1492(*w*)	**C-N** stretching vibrations coupled with the **C-H** bending
1673(*s*)	**Amide I**

Table A-5: The DNA sequences for Probe 1, Target 1, and scrambled Target 1.

	Sequence
Probe 1	5'-/5ThioMC6-D/TCC TGG GCT GGC GGG TCG CTT CC-3'
Target 1	5'-GGA AGC GAC CCG CCA GCC CAG GA-3'
Scrambled Target 1	5'-ACC GAG CCA GGC AGC CAG GGC AC-3'

Table A-6: Peaks present in the Probe 1 spectrum with their corresponding assignment.

Peak (cm^{-1})	Assignment[53]
1644 (*m*)	**Amide I**
1575 (*m*)	**G, A** (ring breathing modes of the DNA/ RNA bases)
1509 (*m*)	**Cytosine**
1478 (*m*)	**C=C**
1348 (*m*)	-
1310 (*w*)	**Amide**
1259 (*w*)	**Guanine, cytosine** (NH$_2$), **Amide III**
1196 (*m*)	**C-NC** (sym. stretch), **OH, O, C-H** (bend), **CH$_3$**
1085 (*m*)	**Phosphodiester groups** in nucleic acids
1018 (*w*)	Sketching **C-O** ribose
958 (*w*)	Symmetric stretching vibration of ν_1
788 (*s*)	**- O-P-O-** phosphodiester bands in DNA, **DNA, O-P-O** stretching
684 (*w*)	**S-C** mode

Table A-7: peaks present in the 12-MDA spectrum with their corresponding assignments.

Peak (cm^{-1})	Assignment[77]
630 (*m/w*)	υ(**C-S**)
704 (*m*)	**CH$_2$** rocking (**-CH$_2$SH**)
927 (*s*)	υ(**C-C**)
1100 (*s*)	**C-C** vibration in gauche-bonded chain
1298 (*m/w*)	**CH$_2$** wagging (-**CH$_2$-S**)
1397 (*w/sh*)	**CH$_2$** deformation, **-C=O** symmetric stretch
1435 (*s/m*)	**CH$_2$** scissoring (**-CH$_2$CO-O**)